Universidade do Minho
Escola de Engenharia

Joana Cristina Almeida Andrade Dias da Costa

Development of high specific strength components, with internal cellular structure, for several applications

novembro de 2015

Joana Cristina Almeida Andrade Dias da Costa Development of high specific strength components, with internal cellular structure, for several applications

UMinho | 2015

Universidade do Minho
Escola de Engenharia

Joana Cristina Almeida Andrade Dias da Costa

Development of high specific strength components, with internal cellular structure, for several applications

Dissertação de Mestrado
Mestrado em Engenharia Mecânica

Trabalho efectuado sob a orientação do
Professor Doutor Filipe Samuel Correia Pereira Silva

novembro de 2015

DECLARAÇÃO

Nome: Joana Cristina Almeida Andrade Dias da Costa
Endereço eletrónico: andradejoana35@gmail.com Telefone: 915280850
Bilhete de Identidade/Cartão do Cidadão: 13789850
Título da dissertação:

Development of high specific strength components, with internal cellular structure, for several applications

Orientador:
Professor Doutor Filipe Samuel Correia Pereira Silva

Ano de conclusão: 2015
Mestrado em Engenharia Mecânica

Universidade do Minho, _____/_____/_____

Assinatura:

ACKNOWLEDGMENTS

This work has been possible thanks to the collaboration of many people within the Department of Mechanical Engineering of the University of Minho.
Inside the Department of Mechanical Engineering, special gratitude is given to Professor Filipe Samuel Silva and Jorge Martins for their support and orientation during this work.
I also would like to thank Engineer Paulo Pinto for his help with the cellular structure drawings.
I would like to thank João Faria, Nélson Lima and Joel Silva, for the help with the 3D printer machine.
I also have to thank to my family, my mother, my father and my grandmother, without them it would be impossible to finish this work. And to my sister and brother, for putting up with me.
I would like to address a special gratitude to my friends, Flávia Barbosa, who helped me with the Word and the Excel, José Grilo and Filipe Pimenta, who gave me support on SolidWorks and finally Ana Carvas, Pedro Silva , Daniel Aires and Beatriz Matos for their friendship.

ABSTRACT

Today's society is characterized as a consumer society in terms of natural resources. In this sense, the most important resources are related to energy and materials. The goal is to try to reduce this excessive consumption of resources. One of the solutions is to turn the use of the raw material more efficient in components, in this case applied to mechanical engineering. The subject of this dissertation, *"Development of high specific strength components, with internal cellular structure, for several applications"*, meets the goal of the material used, thus aiming to reduce the amount of material in areas where it is not being properly employed.

The first step was to choose an iconic component of mechanical engineering, a heavy duty piston. From the original design of that piston is made a static simulation, where the boundary conditions are the result of state of the art. With the results of that simulation it is possible to extract and analyze the areas where stresses are not too high, comparing to the maximum stress. These are areas that are likely to be improved iteratively making the piston lighter than the original. Moreover, a thermal analysis was performed, since the piston is subject to high thermal loads. At the end, the simulations of either the conventional piston or the idealized piston, are compared and the mechanical and thermal properties are kept.

After the computational validation of the new component, proceed to the 3D printing in PLA.

Key words: Cellular Structures, Mechanical Properties, Heavy Duty Piston

RESUMO

A sociedade de hoje é caracterizada como sendo uma sociedade consumista em termos de recursos naturais. Neste sentido, os recursos mais importantes estão ligados à energia e aos materiais. A questão é de tentar reduzir este consumo excessivo de recursos. Umas das soluções é praticar um uso eficiente do material em componentes, neste caso, aplicados à engenharia mecânica. O tema desta dissertação, "*Desenvolvimento de peças de elevada resistência específica, com estrutura celular, para aplicações diversas"*, vai de encontro ao aproveitamento do material usado, visando assim reduzir a quantidade de material em zonas em que o mesmo não está a ser propriamente aproveitado.

O primeiro passo foi escolher um componente icónico da engenharia mecânica, um pistão utilizado em transportes pesados. A partir do desenho original desse mesmo pistão é feita uma simulação estática, onde as condições de fronteira são fruto do estado da arte. Através dos resultados dessa mesma simulação é possível extrair zonas onde as tensões não são elevadas, comparando com a tensão máxima. São essas zonas que são passíveis de ser iterativamente melhoradas tornando o pistão mais leve do que o original. Também foi realizada uma análise térmica, dado que o pistão está sujeito a elevadas cargas térmicas. No final, as simulações, quer do pistão convencional quer do pistão idealizado, são comparadas e as propriedades mecânicas e térmicas são mantidas.

Após a validação computacional do novo componente, procede-se à impressão de ambos os pistões em PLA.

Palavras-chave: Estruturas Celulares, Propriedades Mecânicas, Pistão Para Transportes Pesados.

CONTENTS

LIST OF FIGURES

LIST OF TABLES

ABREVIATIONS AND SYMBOLS

Symbol	Definition	Unit
	Abbreviations	
Al	Aluminium	-
BDC	Bottom dead centre	-
CAD	Computer aided design	-
Cu	Cupper	-
Fe	Iron	-
FOS	Factor of safety	Dimensionless
Mg	Magnesium	
	Roman symbols	
a	Linear acceleration	m/s^2
a_p	Linear acceleration	m/s^2
F_K	Piston force	N
F_S	Lateral force	N
F_{ST}	Rod force	N
h	Convection coefficient	W/m^2K
k	Thermal conductivity	W/mK
l	Length of the connecting rod	m
m	Total of mass	kg
m_{rod}	Mass of the rod	kg
m_{piston}	Mass of the pin	kg
n	Ratio between the length of the connecting rod the crank radius	Dimensionless
N	Angular velocity	Revolutions per second
Nu	Nussle	Dimensionless
Pr	Prandtl	Dimensionless
Re	Reynolds	Dimensionless
U	Oil velocity	m/s
T	Temperature in the combustion chamber	℃

v_{jet}	Jet's velocity	m/s
v_{piston}	Piston's velocity	m/s
x	Piston's position	m
	Greek symbols	
α	Angular acceleration	rad/s^2
θ	Crankshaft degree	rad
ω	Angular velocity	rad/s
ρ	Density	kg/m^3
σ_{limit}	Limit stress of the material	MPa
$\sigma_{vonMises}$	Maximum stress	MPa
γ	Kinematic viscosity	m^2/s
μ	Dynamic viscosity	$Pa \cdot s$

1. INTRODUCTION

This chapter is present a brief explanation on cellular structures as well as the connection between processing, theory, mechanical properties and characterization. It also guarantees the aims, the dissertation layout and the motivation.

1.1 Cellular structures

When modern man builds large load-bearing structures, he uses dense solids: steel, concrete, glass. When nature does the same, it generally uses cellular structures such as: wood, bone, coral. There must be good reasons for it.

The use of cellular structure allows the material to have good mechanical properties as well as low mass. Materials with cellular structure generally occur in nature and have many possible engineering applications. Examples of cellular structures in nature are wood, bone, cork, plant stems, glass sponges and bird beaks. Man has made many synthetic cellular structures, such as honeycomb-like materials used for lightweight aerospace components.

The successful application of materials requires that they satisfy a set of properties. These properties can be thermal, optical, mechanical, physical, chemical and nuclear. Those properties are linked to the structure of the materials and the way of its manufacturing process. A schematic framework that shows the relationship between the four elements: mechanical properties, characterization, processing and theory is present in Figure 1.1.[1]

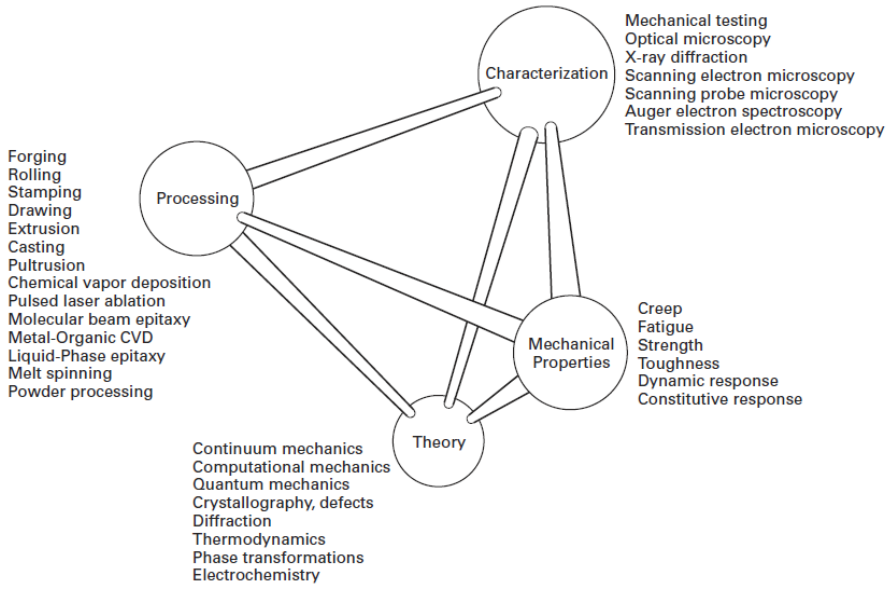

Figure 1.1 Relationship between: Processing, Theory, Characterization and Mechanical Properties [1]

Cellular structures (metal foams, “metfoams” or cellular metals) are a new class of material unfamiliar to mechanical engineers. They are made possible by a range of novel processing techniques, many of which are still under development.[2] At the present, University of Minho has a new technique that makes it possible to produce new lightweight components with cellular structures.

One of the potentialities of the cellular structures is its behavior to compression that, to impact requirements is an important factor. On using this kind of structure is possible to make lower components.[3]

One of the examples of cellular structures is the honeycomb structure. This type of structure is used in airplane, ship and automobile constructions. The design is achieved with two thin walls and the honeycomb structure between them, see Figure 1.2.

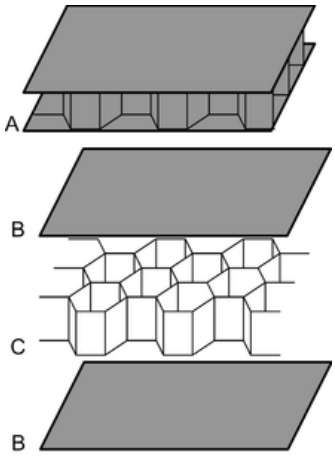

Figure 1.2 Honeycomb structure [2]

1.2 Scope and structure of the thesis

This dissertation is concerned with the development of an optimised piston based on a conventional piston and also a static analysis and a thermal analysis in order to compared them with each other and validate the final CAD model.

This work is elaborated in 5 chapters. Chapter 2 deals with the state of the art, in order to define the boundary conditions for the study. This chapter is designed to give the readers with different backgrounds to a common level of knowledge. The main covered topics are: the 1) Piston terminology, 2) Piston as a component of power transmission, 3) Mechanical loads, 4) Thermal loads, 5) Piston materials, 6) Methods of cooling, 7) Processes of manufacture, 8) Piston types.

The third chapter contains the methodology, is devoted to the piston mas optimisation with the main analysis, thermal and mechanical. It covers 8 sections: 1) Design (chosen piston), 2) Analysis of the slider-crank mechanism, 3) Static analysis – conventional piston, 4) Thermal analysis – conventional piston, 5) Optimisation, 6) Static analysis – optimised piston, 7) Thermal analysis – optimised piston and 8) results.
The fourth chapter, named as Manufacture process, mainly describes the 3D printing process.
Finally, Chapter 5, encompasses a list of future work and the main conclusions are drawn.

1.3 Motivation

Having the possibility of applying an existent lightweight cellular structure to an iconic mechanical component, a piston, was a challenge.
Knowing that pistons are components with severe requirements, due to structural and thermal operating conditions, was the major motivation on this work. Studying how they have developed and understand how they work fulfilled many engineering fields, from computer aided design and simulations to the manufacture process.
The basic requirement for the successful fulfilment of the function of a structure is that the working stresses in critical sections, cannot exceed the allowed limit of the material. The request of lightweight design is to use maximal available material resources with the minimum mass. Therefore, having the opportunity of change a conventional piston and optimised it, reducing its mass, was a motivating challenge.

1.4 Aims

The purpose of this work is to design a heavy duty piston using some of the properties of cellular structures in order to reduce its mass in 30%. The specific aims of this work are:

- Design a new heavy duty piston, applying a cellular structure, through an existent conventional piston;
- Perform a static analysis on the conventional piston and from that data redesign an optimised piston;
- Perform a thermal analysis on both pistons;
- Make a prototype of both of the pistons.

2. STATE OF THE ART

Engine piston is one of the most complex mechanical component among all automotive field. Piston materials and its design have been under development during the years and it will be that way until fuel cells, exotic batteries or another thing that can replace the conventional way of energy transformation on an engine. [4]

2.1 Piston terminology

Functional divisions of the piston are the crown, the ring belt with top land, the pin boss and, finally, the piston skirt, see Figure 2.1 . There are more elements on pistons, such as cooling galleries and ring carriers that specifies the type of piston design. [5]

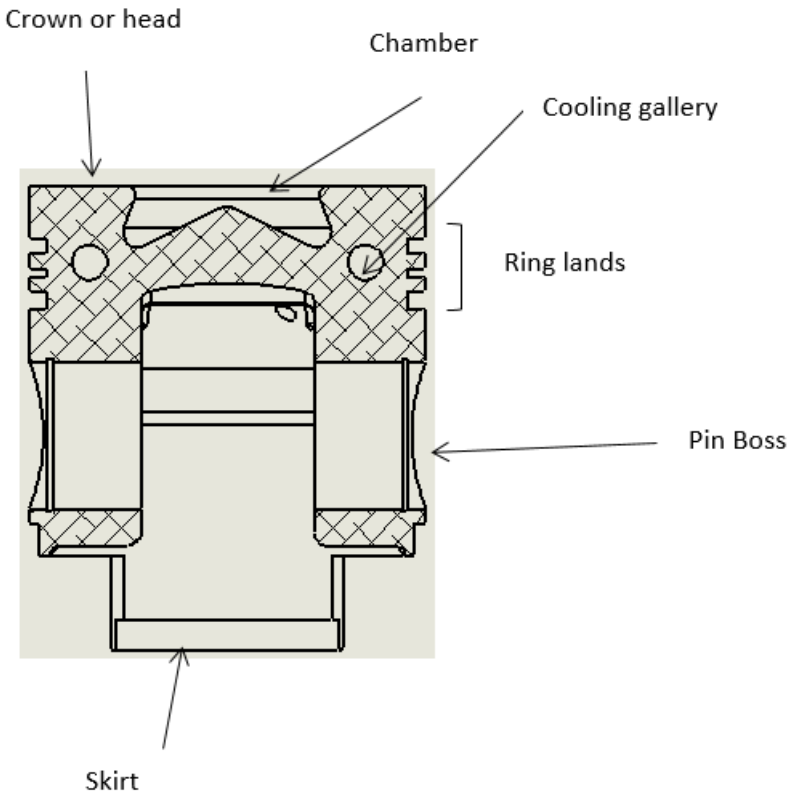

Figure 2.1 Piston terminology

The upper part, or top, of the piston is named the crown, and it is exposed to the cylinder chamber and, therefore, the effects of the pressure and heat from the combustion.
The circumferential edge of the piston, around the crown, is known as its leading edge.

The piston head or crown forms the cavity of the combustion chamber. For diesel and gasoline pistons, the combustion chamber comes in different geometries, due to the number and location of the valves, see Figure 2.2. [5]

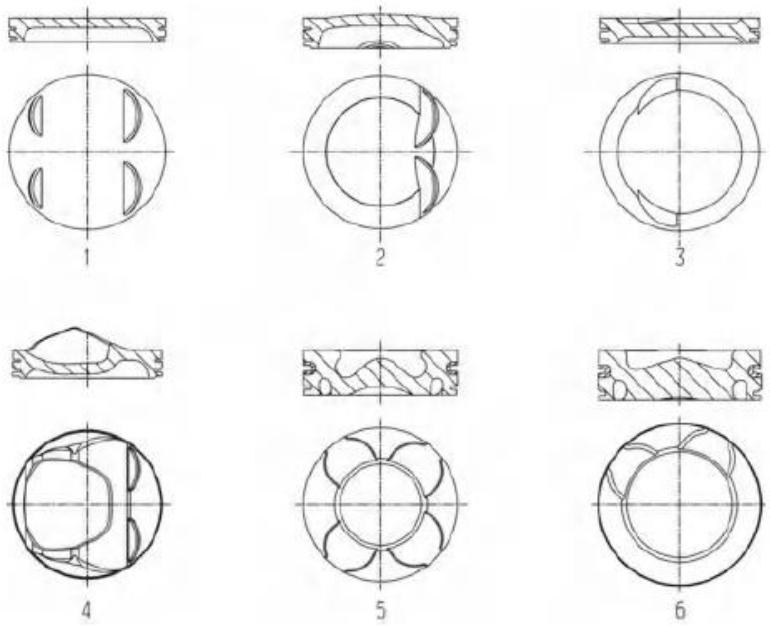

Figure 2.2 Types of piston crowns (1-3 for four-stroke gasoline engines with multi-point injection, 4 for four-stroke gasoline engines with direct injection, 5-6 four-stroke diesel engines with direct injection) [5]

The piston ring belt is divided in three ring grooves that are made to hold the piston rings. There are two basic types of piston rings. The top two rings are the compression rings, which are designed to seal the expanding gases in the combustion chamber. The third ring is responsible to control the oil, it must scrape the oil down the cylinder walls and prevent it from entering the combustion chamber.

The pin bore, or pin boss, sliding mechanism must be in the highest condition in order to keep the engine in reliable conditions. If the surface roughness is too low this can cause galling of the pin bore. Some pistons use bearing and bushings, see Figure 2.3, its primary function is to support the moving parts while absorbing and transferring occurring forces. [6]

Figure 2.3 Bearing and bushings [6]

The piston skirt is the part of a piston that extends the lowest. It is tasked with keeping the piston from shocking excessively in the cylinder. It is typically machined with small grooves to help in holding and transporting oil to the cylinder walls to provide proper lubrication. In some high-performance applications, the piston skirt may be coated with a type of material which aids in lubrication and prevents scuffs from occurring on the cylinder wall. On Figure 2.4 is possible to see 3 different types of skirt's shape. [6]

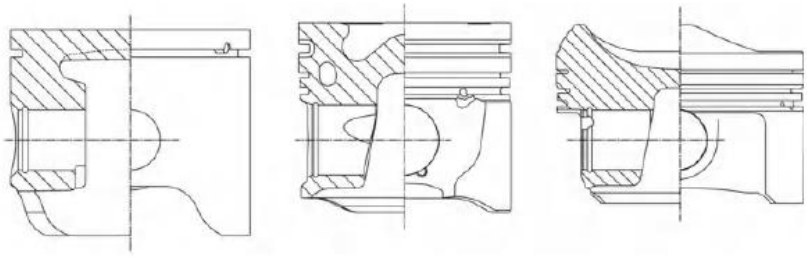

Figure 2.4 Skirt shapes [6]

2.2 Piston as a component of power transmission

In a cylinder engine, the energy bound up in the fuel is quickly transformed into heat and pressure during the combustion cycle. The heat and pressure values rise critically within a very short period of time. The piston, as a moving component of the combustion chamber, is in charge of converting this released energy into mechanical work.[6]

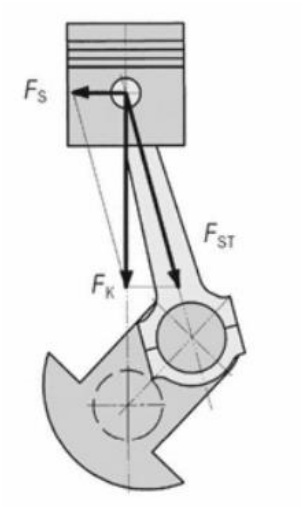

Figure 2.5 Forces on the piston [6]

The gas pressure pushed against the piston head and the oscillating inertial forces of the piston plus the connecting rod constitute the piston force (FK). Due to the redirection of the piston force in the direction of the rod (rod force FST), an additional component ascends – following the force parallelogram – known as the lateral force FS, or normal force. This specific force presses the piston skirt against the cylinder bore. Shown in Figure 2.5 and Figure 2.6. [6]

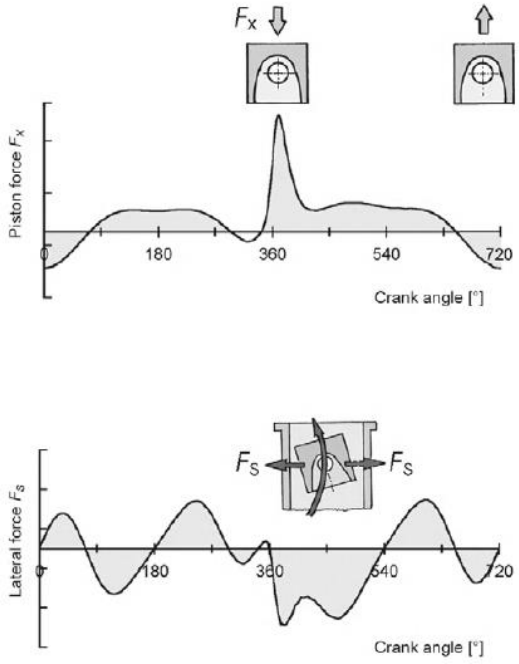

Figure 2.6 Force graphic [6]

As a moving and force-transmitting part, the piston, with the piston rings, must conveniently seal the combustion chamber against gas passage and the penetration of oil under all load conditions. This task can only be fulfilled if a hydrodynamic lubricating is between the piston rings or skirt and the cylinder bore. The stoppage of the piston at the two dead centre points (top dead centre and bottom bead centre), where the oil is not correctly functional, is particularly critical.[6]

It is now presented the most important tasks that the piston must achieved, such as:

- Transmission of force from and to working gas;
- Sealing off the working chamber;
- Linear guiding of the connecting rod; (trunk piston engines)
- Heat dissipation;
- Controlling charge exchange; (in two strokes engines)
- Guiding the sealing elements; (piston rings)
- Guiding the connecting rod. (for top-guided connecting rods)

Pistons have to fulfil many different tasks such as:

- Structural strength;
- Adaptability to operating conditions;
- Low friction;
- Heat dissipation;
- Low wear;
- Seizure resistance and simultaneous running smoothness;
- Low weight with sufficient shape stability;
- Low oil consumption ;
- Low pollutant emissions values.

This requirements are, in part, contradictory, both in terms of design and material. These conditions must be carefully coordinated for each engine type. The optimal solution can therefore be quite different for each individual case. [6]

2.3 Mechanical loads

The cyclical loading of the piston is due to:

- The gas pressure from de cylinder pressure;
- The inertia force from the oscillating motion of the piston;
- The lateral force from the support of the gas force by the inclined rod, and the inertia force of the oscillating connecting rod.

The simulation of the gas force is intended to represent the effect of the gas pressure on the piston ate the top dead centre position. The gas pressure is applied to the CAD model over the entire piston crown.

The oscillating motion of the piston in the cylinder generates accelerations that reach the maximum at the top dead centre. In this context, the length of the rod relative to the crank radius pin, also known as the stroke-connecting rod ratio, plays a big role. As the length of the rod increases, the acceleration of the piston and the lateral forces decrease. Maximising the length of the connecting rod becomes by means one design principle. The accelerations are linearly dependent on the stroke-connecting rod ratio of the crank mechanism, and quadratically dependent on the engine speed. This means that the effects of the inertia are greats in high speed engines.[6]

2.4 Thermal loads

The thermal loads on the piston result from the combustion process with peak gas temperatures, in the combustion chamber, between 1700 and 2600℃ depending on type of engine, fuel, gas exchange, compression, and fuel/gas ratio.

The process of combustion is mainly transferred to the piston walls and the piston top by convection. The heat is then dissipated through the water cooling system of the chamber and by the oil existent on the gallery and on the piston walls.

The resulting temperature profile within the piston is shown in Figure 2.7.[7]

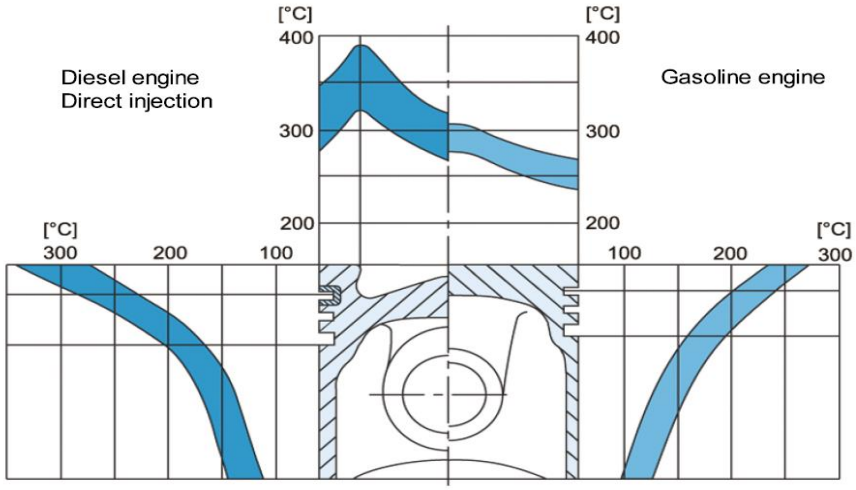

Figure 2.7 Temperature profile of diesel and gasoline pistons [6]

2.5 Piston materials

Besides their design shape, the strength of the material is an important factor for the load capacity of the component. Loads, static and dynamic, are changing over the years, due to the improvement on the engines. Temperature resistance is also a main factor, due to the high thermal loads.

The thermal conductivity of the chosen material is crucial for the maximum temperature that the material can hold.

Static and dynamic strength values describe material behaviour under isothermal condition, which means that the temperature is constant. Pistons are exposed to high temperatures during power train contents. The transient heat loads sometimes ascend the elastic limit. Materials must also be resistant to those stresses.[7]

2.5.1 Aluminium

Pistons are almost exclusively made of aluminium-silicon alloys of eutectic, and some hyper eutectic composition, which can easily and nearly always can be forged as well.

Aluminium alloys are the preferred material for pistons, gasoline and diesel, due to their mechanical properties: low density, high thermal conductivity, simple net-shape manufacture techniques, easy machinability and great recycling characteristics. Forged pistons from eutectic

and hypereutectic alloys reveal higher strength and are mainly used in high performance engines.[8]

Alloys with a silicon percentage below 12.5% are named hypoeutectic, and those with a content higher than 12.5% are hypereutectic, see Figure 2.8. [7]

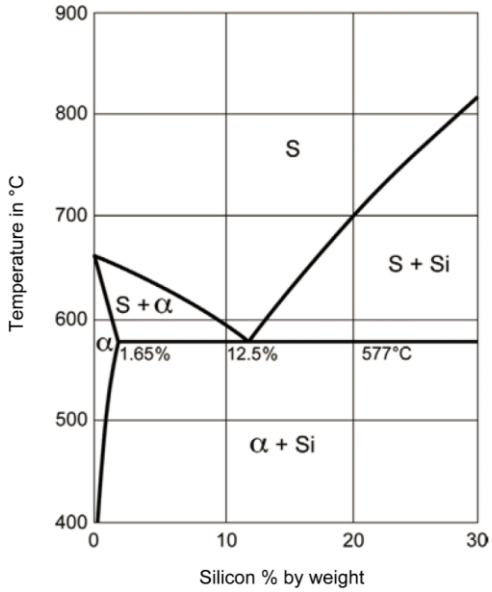

Figure 2.8 Phase diagram AlSi [6]

2.5.2 Ferrous materials

If the strength or wear resistance of aluminium alloys is not satisfactory to meet the mechanical or thermal loads, then ferrous materials are applied. This can be with only a local reinforcement or be extended to parts of composite pistons, all the way to piston built entirely of cast iron or forged steel.

Cast iron materials, generally, have a carbon content of > 2%, see Figure 2.9. In these materials, the inelastic cementite or graphite can no longer be brought into solution by subsequent heat treatment. They are therefore not appropriate for hot radical forming, but their castability can be improved.

For the materials used in piston casting, the basic material of the structure is mostly perlitic, due to its good strength and wear properties.

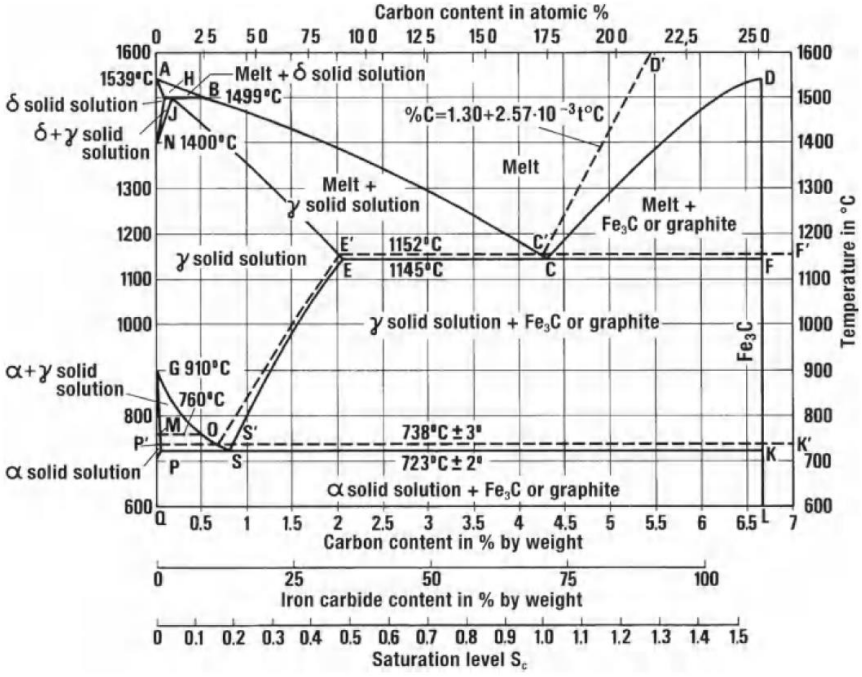

Figure 2.9 Phase diagram FeC [6]

The iron alloys also known as steels have a carbon content of less than 2%. When heat-treated, they became suitable for forging. The steels are an excellent material for hot forming, unlike the iron materials.

Steels used for pistons, generally, have a carbon content less than 0.8%. If they are cooled slowly after casting or hot forming, the ferrite-perlitic structure is formed. [6]

At first sight the temperature strength of steel suggests that the material is the best choice for high performance passenger car Diesel engines. However, Al conducts heat three times better than steel, which is why the steel pistons can reach temperatures 50 to 100 ℃ hotter than the Al pistons. Higher temperatures leads to a hotter gallery, which can cause the oil to crack. Carbon that results from this cooking process starts to form a layer on the cooling gallery which can impact the cooling process. To solve this problem, steel pistons tend to have bigger galleries, see Figure 2.10, to ensure a sufficient oil flow.[9]

Figure 2.10 Representation of a Steel and an Al piston, on the left a Steel piston and on the right an Al piston [9]

2.6 Methods of piston cooling

The size of the piston, peak cylinder pressures and whether the engine is turbocharged or not all determine what kind of cooling system is required. Within the same group of engines, it is possible to find different types of cooling depending on the power of the engine. Lower horsepower engine specifications do not use cooling jets and those with higher horsepower trim do.

The piston can be cooled by oil, water or air. Water cooled pistons have been applied to heavy duty, low-speed engines for a while, but more recently it seems to have been dropped because of the serious design and maintenance challenges with the piping and sealing. Though, this type of cooling has some advantages, since the water has a higher specific heat and a lower viscosity than oil therefore heat transfer takes place. Air cooling is the simpler way in terms of design, but the lower specific heat calls for very large quantities of air to supply the system. This involves heavy pipes, channels and an additional air compressor. The modern method is oil cooling, in which oil can be taken from the main lubrication system along the connecting rod directly to the piston, or from a different place to the piston, which then can be freely released to return to the crankcase.[5]

2.6.1 Pistons without piston cooling

Pistons without a cooling system are mainly used in gasoline engines due to their low thermal loads. They are applied in diesel engines with low output. The temperature profile of these kind of pistons, without a system cooling, can reach 20℃ more than a piston with spray jet cooling. [6]

2.6.2 Pistons with spray jet cooling

The easiest way to cool a piston is by means of spray a jet cooling. A stationary cooling jet is placed in the cylinder bottom just below the cylinder liner. The jet is fed by engine lube under pressure. The oil is shoot against the underside of the piston in order to cool the piston crown and may also lubricate the wrist pin. This technology is mostly applied to gasoline pistons because their low compression height does not allowed a place for a cooling channel. The Figure 2.11 shows a cross section of a piston with no cooling channels. [6]

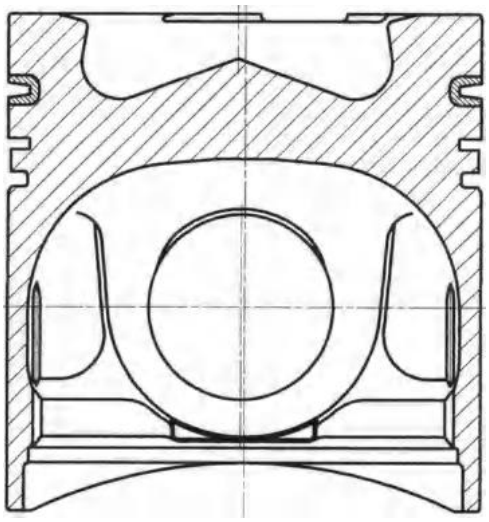

Figure 2.11 Piston without cooling gallery [6]

2.6.3 Pistons with cooling channels

If the piston temperature is not low enough without cooling channels, then cooling channels must be applied. The oil is continuously run through the cooling oil channel during operation Under engine operating conditions, complete filling of the cooling channel is not possible, and the cooling channel moves with the piston up and down, which leads to a turbulent flow rising the heat transfer coefficient.

Depending on the manufacture process, cooling channels are available as salt core cooling channels, see Figure 2.12 on the left, cooled ring carriers, see Figure 2.12 on the right, and machined cooling channels. [6]

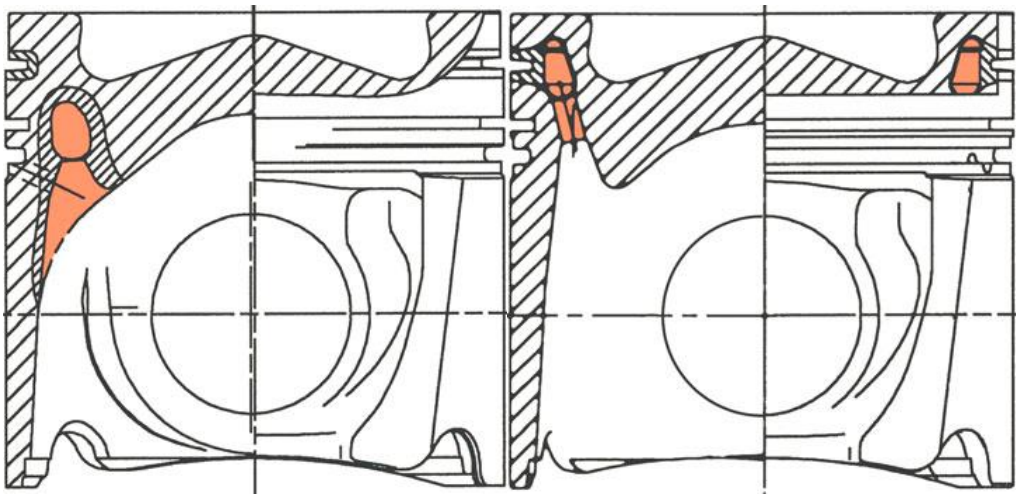

Figure 2.12 Salt core cooling channel on the left, piston with cooled ring carrier on the right.[6]

The next table, Table 2.1, shows a summary of the requirements of pistons as well as some solutions that have been implanted during the years is order to solve some problems due to operating conditions, thermal and mechanical loads.

Table 2.1 Operating conditions and solutions approaches for piston design and material[6]

Operating conditions	Requirements on the piston	Design solution	Material solution
Mechanical Load 1. Piston crown/combustion Max. gas pressure gasoline engine: 3.5 – 8.0MPa Max. gas pressure, four-stroke gasoline engine : Naturally aspirated gasoline engine: 6.0-9.0 MPa Turbo: 9.0-12.0 Mpa Naturally aspirated diesel engine: 8.0-10.0 Mpa Turbo: 14.0-24.0 MPa 2. Piston skirt Lateral force: approx. 10% of the max. gas force 3. Pin boos Permissible surface temperature-dependent	High static and dynamic strength, even at high temperatures	Sufficient wall thickness, shape stable design, consistent force flow and heat flow	Various AlSi casting alloys, warm aged (T5) or age hardened (T6), cast or forged; Forged steel Specialty brass or bronze bushings
Acceleration of the piston and connecting rod at high rpm: partly much greater than 25 m/s^2	Low mass, resulting in small inertia forces and inertia torques	Lightweight construction with ultra-high material utilization	AlSi alloy, forged
Sliding friction in the ring grooves, on the skirt, in the pin bearings; at times poor lubrication conditions	Low frictional resistance, high wear resistance (affects service life), low seizing tendency.	Sufficiently large sliding surfaces even pressure distribution; hydrodynamic piston shapes in the skirt area; groove reinforcement	AlSi alloys, tin plated, graphite coated skirt, groove protection with cast-in ring carrier or hard anodizing
Contact alteration from one side of the cylinder to the other	Low noise level, moderate “piston tipping” in cold or warm engine, low impulse loading	Low running clearance, elastic skirt design with optimized piston shape, pin bore offset	Low thermal expansion. Eutectic or hypereutectic AlSi alloys.

2.7 Processes of Manufacture

The manufacture of the raw part should be as near to net shape as possible, and should contribute to high material quality. Usually a piston is made either by casting or forged process. The sliding and sealing surfaces require high-precision finishing, which demands suitable machinability of the material. [6]

2.7.1 Gravity die casting

Casting is a manufacturing process by which a molten material such as metal is introduced into a mould, allowed to solidify within the mould, and then ejected or broken out to make the manufactured component. Gravity die casting is one of the standard processes for the manufacture of high-integrity automotive castings. It represents proven and absolute precision technology for the production of large batch quantities.

Good heat dissipation from the solidification casting through the dies leads to short solidification times. This results in casted parts with good mechanical properties, especially after an additional heat treatment.[10]

2.7.2 Closed die forging

In the other hand, pistons can be made through forged process. Forging is the term for shaping metal by plastic deformation. Cold forging is done at low temperatures, while conventional hot forging is made at high temperatures. They are made from higher strength aluminium alloy billets which are compressed into their primary shape rather than poured.

Either of the processes requires finish processes of manufacture. Such as: [11]

- Pin boring;
- Turning;
- Finish processes and
- Pin Fitting and final inspection

The majority of the pistons are casted, however forged pistons present better mechanical properties due to the grain size. High performance pistons are forged due to lower thermal conditions and higher velocities. [12] In Figure 2.13 it is shown a Formula 1 forged piston.

Figure 2.13 Forged piston for Formula 1 [6]

2.8 Piston Types

The countless operating criteria of combustion engines opens to a wide variety of engine types, which leads to a big amount of pistons types, because each engine has its own requirements characterised by its construction, shape, dimensions and material.

At this point, the main topics are pistons for gasoline engines and pistons for diesel engines. Those main topics are split into processes of manufacture and specific developments due to its requirements, thermal and mechanical loads.

The pistons made for gasoline engines are present in Figure 2.14 and the diesel pistons are shown in Figure 2.15. Both of them have develop due to the increase of the thermal and mechanical loads. Gasoline pistons tend to be lighter than the Diesel pistons due to the requirements (much higher speeds), Diesel pistons achieve higher temperatures than the gasoline pistons and the gas pressure it is greater in Diesel pistons. [7]

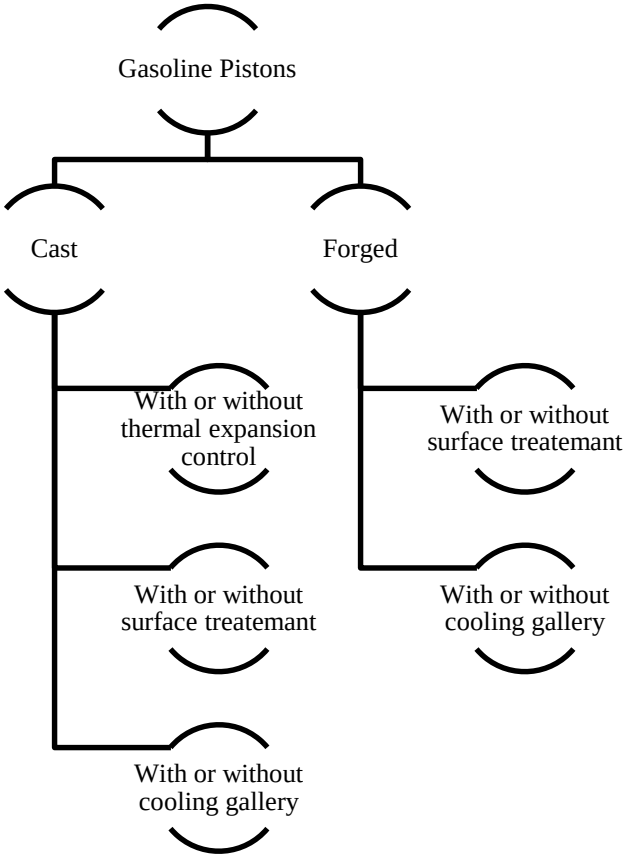

Figure 2.14 Gasoline pistons [7]

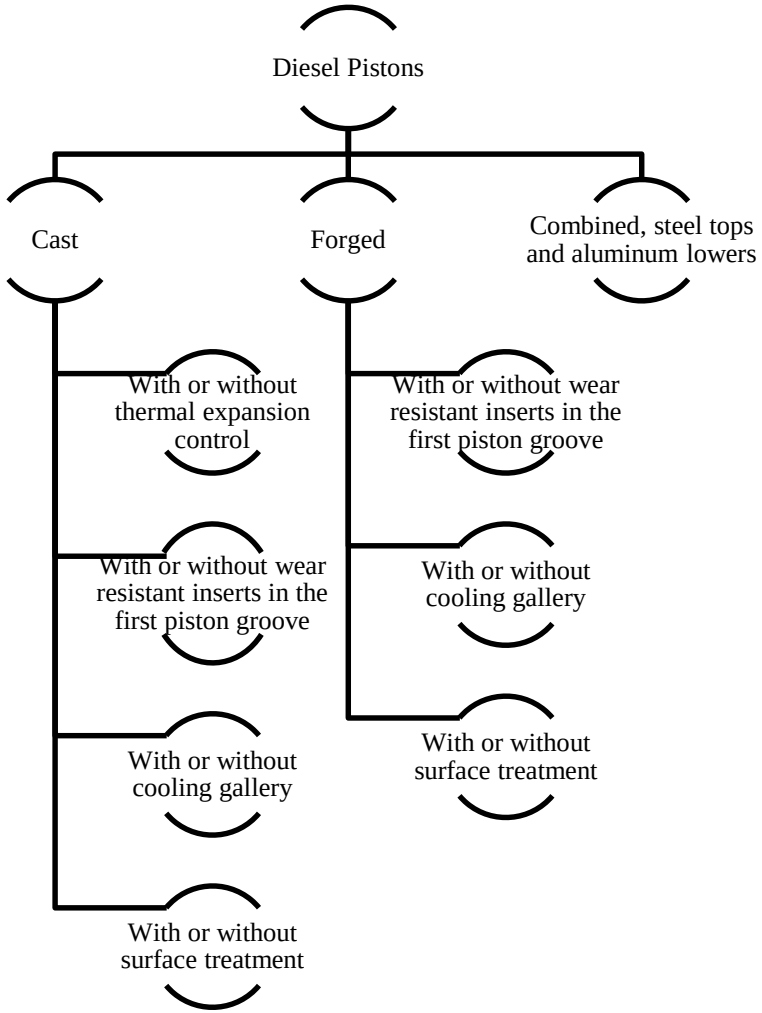

Figure 2.15 Diesel pistons [7]

2.8.1 Thermal expansion control

These type of piston have insert strips that control thermal expansion, see Figure 2.16. They are placed in grey cast iron crankcases. The main goal of these piston design, and very many inventions in this field, is to reduce the relatively large differences in thermal expansion between the cylinder and the aluminum piston.[6]

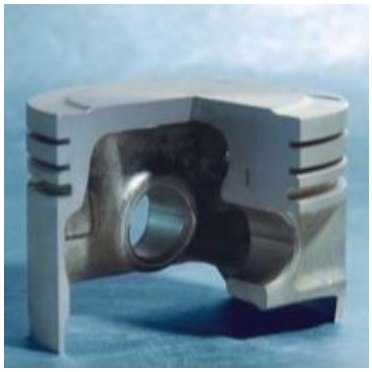

Figure 2.16 Thermal expansion control [13]

Steel or ceramic cast-in parts are used as local reinforcements to control the thermal expansion, reducing the main effects of different expansion coefficients in contact areas with two different materials. When used iron engine blocks, the thermal expansion control of aluminium pistons is, usually, controlled by steel inserts in the pin boss area.

2.8.2 Surface treatment

Surface treatments are made in order to create good tribological conditions for the pistons. Coating of the piston skirt is a mainly to prevent local welding between the piston and the cylinder, or piston seizing. A wear protective coating is not needed in this connection.
In Figure 2.17 is present three different zones where the surface can be treated. The first is to improve the endurance between the piston and the cylinder. The second the molibdemum coat is added to improve the lubrication of the piston. And the last, is applied on the crown for better resistant to heat.[6]

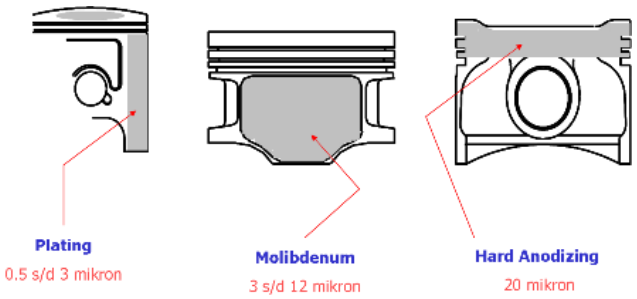

Figure 2.17 Wear resistant surface [8]

Usually, in moderate running conditions, a piston does not require a coated skirt if its dimensions are designed careful and correctly. Danger of seizing does exist, under extreme operating conditions:

- Lack of local clearance, caused by mechanical and/or thermal deformation of the cylinder;
- Insufficient lubricant;
- Brand new condition, when the cylinder-piston have not yet run in.

Usually coats for piston skirts of all sizes are made of fine graphite particles fixed in a polymer matrix. It withstands temperatures up to 250 ºC that it is probable to occur in piston skirt and is resistant to oils and fuels. The film-forming polymer matrix supports the action of the solid graphite lubricant during dry running, with great tribological properties. This offers great seizure resistance for very low clearances and absence of oil.[6]

2.8.3 Cooling gallery

A closed gallery piston includes a piston body having an inside placed for cooling oil defined by two walls, the bottom wall and the outer wall of the piston body, see Figure 2.18. The gallery is formed in the bottom of the wall to house a flow of cooling oil. The oil gallery boss rather joins with the outer wall to provide a greater structural integrity to the piston body.

Figure 2.18 Cooling gallery [6]

2.8.4 Cooled ring carrier

The pistons with cooled ring carrier, Figure 2.19, is an improved way to cool the piston of diesel engines. This cooling system improves the heat dissipation of the first piston ring groove.
A cooled aluminium ring carrier piston from *Mahle* was developed for the heavy-duty range of commercial vehicle diesel engines with peak cylinder pressure of 20 MPa. Features include use of high-temperature-resistant aluminium alloy and a cooled ring carrier to further extend service life and lower the bowl edge temperature by up to 30ºC. Other advantages include improved oil consumption, blow-by, and appearance of the pistons as well as production-tolerant dimensions. The Figure 2.19 shows where the ring carrier is placed.[7]

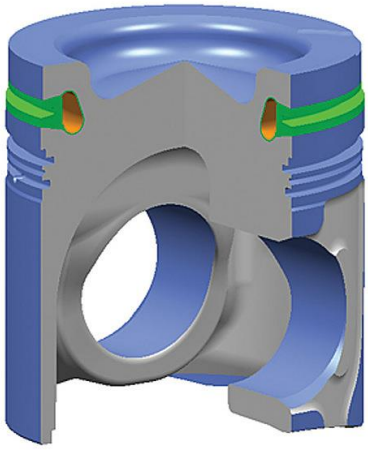

Figure 2.19 Piston with cooled ring carrier [8]

2.8.5 Combined pistons

Ferrotherm is a two-piece piston that had a steel crown with two thin pin boss hoops, and an aluminum skirt that slipped in, see Figure 2.20. The pin holds the whole thing together.
The piston crown, predominantly made of forged or cast-steel, takes on the sealing function together with the piston rings. The crown guarantees minimum wear. The gas forces are also transmitted to the crank mechanism via the piston crown.

Figure 2.20 Combined, or articulated piston [6]

The piston skirt takes over and transfers the lateral forces on the cylinder wall. It is flexibly connected to the piston crown by the piston pin.

2.8.6 Wear resistant inserts in the first piston groove

The manufacture of internal combustion engines with high compression ratios has demanded the use of piston made of aluminum or aluminum alloys in order to get a high conductivity of heat through the crown and downward to the lower portions of the piston. The main problem is that the piston rings tend to deform over the repetitive stress leading to a short piston life. The solution is to create a reinforcement ring, see Figure 2.21, to provide a better performance. As a rule, the ring insert consists of an austenitic cast iron with lamellar graphite.[14]

Figure 2.21 Piston with wear resistant inserts in the first groove [8]

2.8.7 Steel pistons

In diesel engines, steel pistons provide significant potential for reducing CO_2 emissions in comparison with the aluminum pistons, so steel pistons have been developed for passenger car diesel engines to the point of series production readiness. Significant advantages result from the frictional loss. Thermodynamic conditions additionally result in advantages in combustion that lead to a reduction in fuel consumption and emissions levels. The lower compression height of a steel piston can also be utilized to increase the swept volume or to decrease the height of the engine. In Figure 2.22 are present some steel pistons, made by *Mahle*. [6]

Figure 2.22 Steel pistons, by Mahle [6]

The internal-combustion engine's lasting relevance is due to the continuous evolution of its components. Pistons are not sexy. They are not as modish as a lithium-ion battery, as complex as a dual-clutch transmission, or as interesting as a torque-vectoring differential. Yet after more than a century of automotive progress, reciprocating pistons continue to produce most of the power that moves us.

3. METHODOLOGY

This section aims to explain the methodology that was used during this dissertation. The aim of this work is to optimise the weight, less 30 % of its initial weight, of a heavy duty Diesel piston. The optimisation has been carried out by an iterative process, each design alteration was simulated in order to make sure that the new piston has the same, or better, structural and thermal requirements as the conventional.

Each step will be disclosed during this chapter. It will start with a brief description of the old design, and then all the static and thermal analysis. The main data will be presented and explained on the following sections.

The next scheme, shows the the process which was used and adapeted in order to meet the goals of this disseration, the first thing was to define the restrictions and what is possible to change. The first restriction is the material, it has to be the same. Another restriction is the outside geometry, the aim of this project is to reduce weight of a piston but the requirements must be kept, then the outside geometry of the convectional and the optimised piston must match.

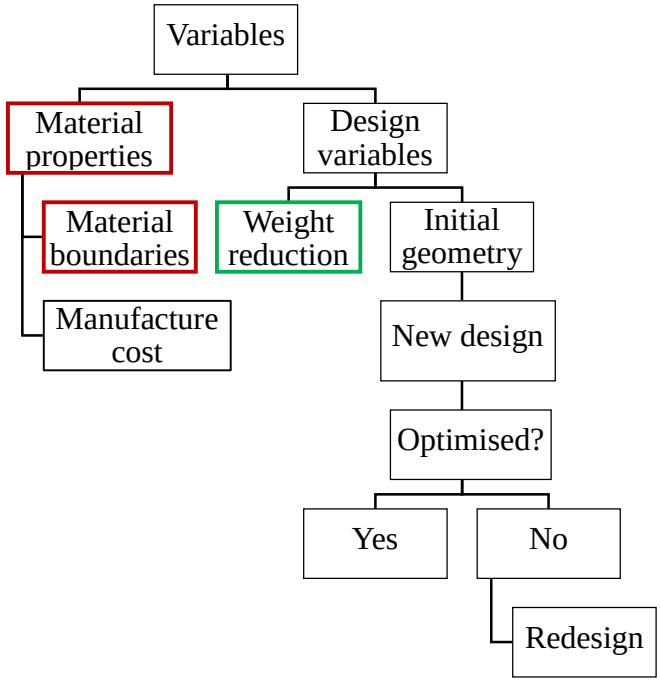

Figure 3.1 Iterative process

The red boxes, material properties and material boundaries, are constraints, which means that cannot be changed. The piston has to be made in the same material and the requirements are the same in both of them. The manufacture cost is not evaluated. The only thing that can be changed is the inner geometry and the wall thickness.

3.1 Design

The first step was to choose and design a heavy duty Diesel piston, performed with SolidWorks™ software. The chosen piston was a heavy duty piston, made of aluminium. The next figure, Figure 3.2, shows the 3D (three dimensions) design. There were three reasons to choose this piston:

- Heavy duty piston as proposed since the beginning of the dissertation;
- One part piston, there are heavy duty pistons made by two parts;
- Data about the piston dimension as well as the piston rod.

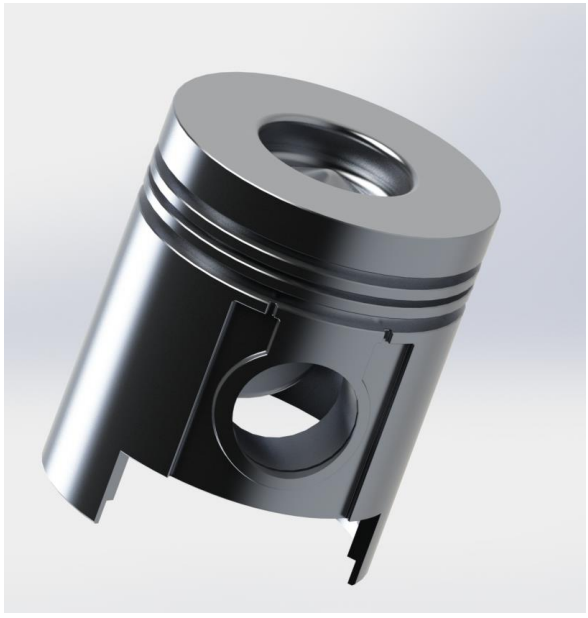

Figure 3.2 Heavy duty piston

As it was said before, the main dimensions, such as the height of the inserts of the pistons rings must be the same. The next table, Table 3.1, shows the dimensions that must be kept during the optimisation process. While the Table 3.2 shows the volumetric properties of the piston, the main goal is to reduce 30% of the mass, so the final weight should be around 1.665 kg.

Table 3.1 Main dimensions of the piston

Features	Dimensions [mm]
Lenght	158
Bore	135
Ring Belt [mm]	
First insert	6
Second insert	4
Third insert	5
Pin Boss diameter	50

Table 3.2 Volumetric properties

Volumetric properties	
Mass	2.3791 kg
Volume	8.88×10^{-4} m^3
Surface Area	0.157 m^2

3.2 Analysis of the slider-crank mechanism

The base of dynamic mechanism operation of engine is slider-crank mechanism, which consist of crankshaft, a connecting rod, a pin and a piston. Combustion pressure transferred from piston (the part merely has reciprocating motion) to the connecting rod (the part has both linear and rotation motion) and finally to the crankshaft (the part that only has rotation motion).

The Figure 3.3, shows a scheme of a slider-crank mechanism with the variables. [15] The x is a representation of the piston displacement, while ω and α are angular velocity and acceleration, respectively. The length of the connecting rod is represented by l , θ is the crank angle, from 0 to 2π rad.

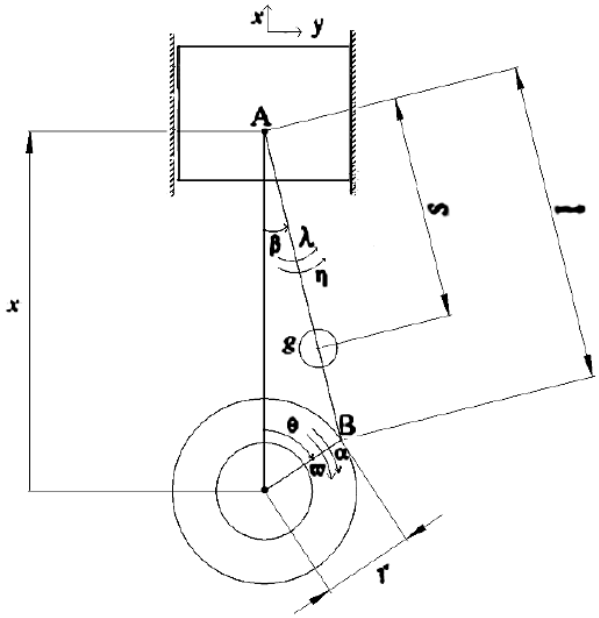

Figure 3.3 slider-crank mechanism [16]

The piston has a linear motion in x direction predicted with the equation 4.1, where $\theta$the crank angle and *r* is its radius. The length of the rod is 0.189 m and the crank radius is 0.063 m.

$$x = r(1 - \cos(\theta)) + (n - \sqrt{n^2 - \sin(\theta)^2}) \tag{3.1}$$

The piston linear velocity is computed with equation 3.2, w is the angular velocity in revolutions per minute (rev/min) and *N* in the angular velocity in rotation per second (rev/s), and *n* is the ratio between the rod length and the radius of the crank. In this study the angular velocity is 2000 rev/min, which means 33.3 rev/s. *C* is the pistons stroke.[12]

$$V_p = V_{average} \cdot \frac{\pi}{2} \cdot sen(\theta) \cdot (1 + \frac{\cos(\theta)}{((n^2 - sen(\theta)^2)^{0.5}}) \tag{3.2}$$

Where,

$$V_{average} = 2CN \tag{3.3}$$

$$N = \frac{w}{60} \tag{3.4}$$

$$n = \frac{l}{r} \tag{3.5}$$

The linear acceleration is calculated through equation 3.6.

$$a_p = N^2 r \cdot (\cos(\theta) + \frac{\cos(2\theta)}{n}) \tag{3.6}$$

From the equation 3.1 it is possible to compute the positions of the piston between the TDC (top dead centre) and the BDC (bottom dead centre).

Piston position is a measure of how far the piston is down the cylinder from its TDC point. The position of the piston can be determined from the crank angle from Top Dead Centre, knowing the stroke of the engine, length of the connecting rod (l) and the angle of the crank. As the crank Shaft rotates a certain degree, the piston moves a certain distance from Top Dead Centre.

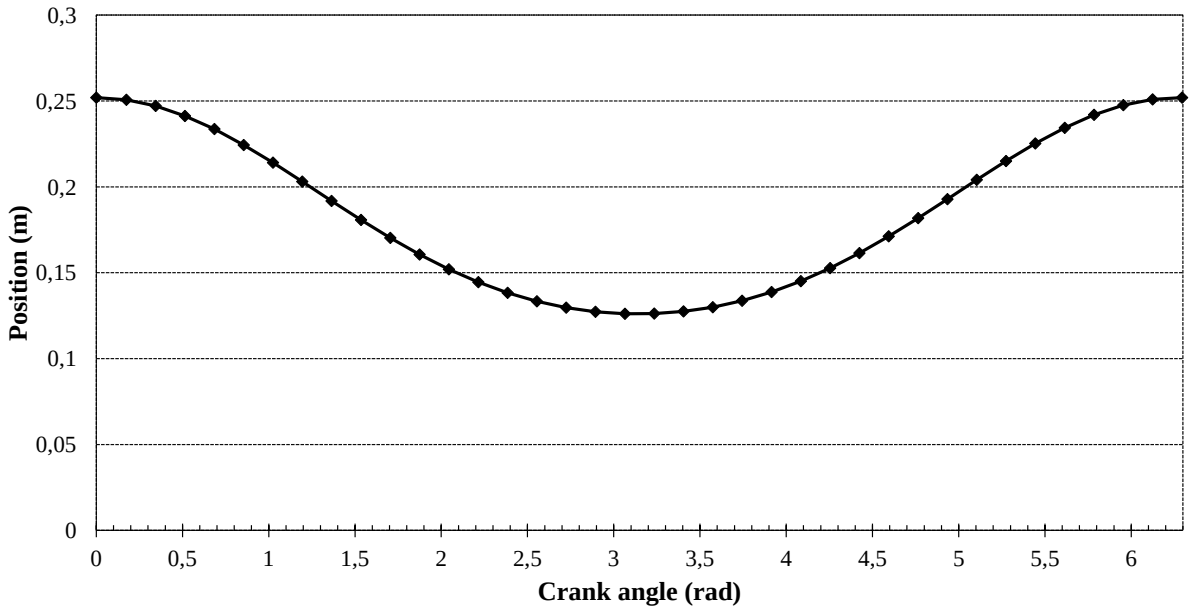

Figure 3.4 Piston position graphic

From the equations 3.2, 3.3, 3.4 and 3.5 the linear velocity of the piston was computed. The results are present in Figure 3.5, the maximum of velocity is reached between the TDC and BDC position, and the minimum is reached between the BDC and the TDC position.

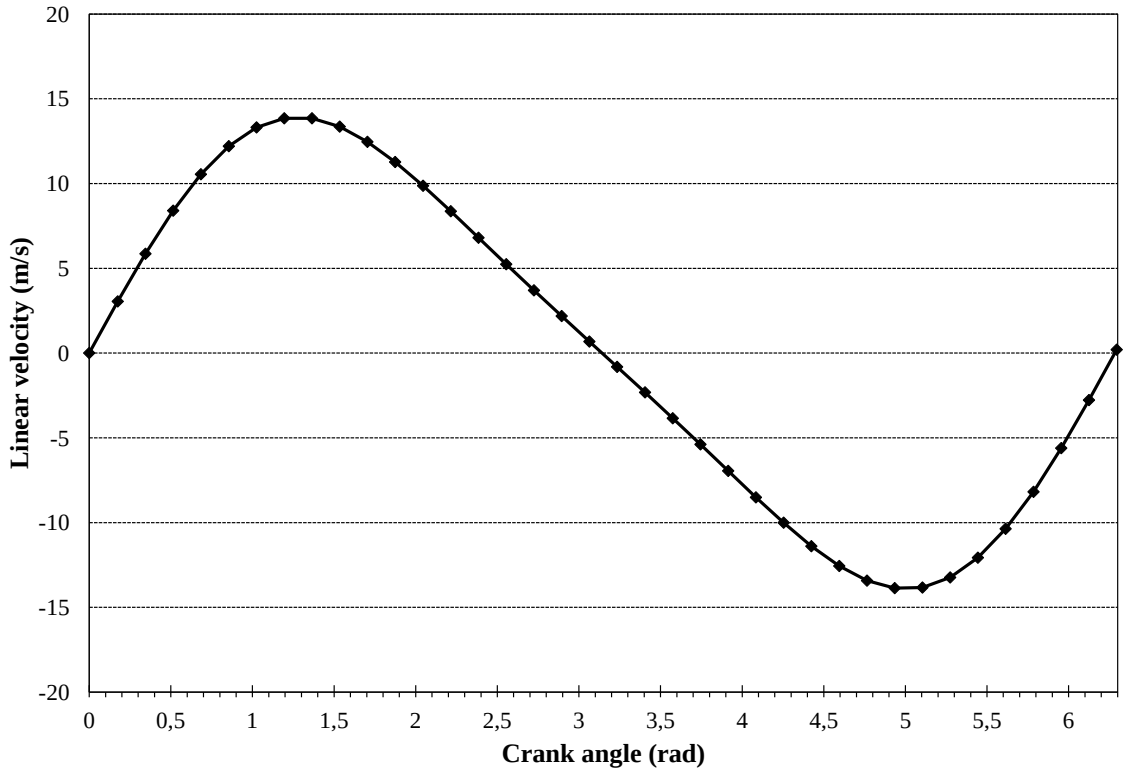

Figure 3.5 Linear velocity graphic

In this study the angular velocity is constant, 2000 rot/min, that means there is no angular acceleration, the Figure 3.6 presents the results achieved through the equations 3.2, 3.3 and 3.8. The maximum of linear acceleration is at TDC position, and the value is 3660 m/s^2, then drops until the BDC position where the value of 1948 m/s^2 is reached.

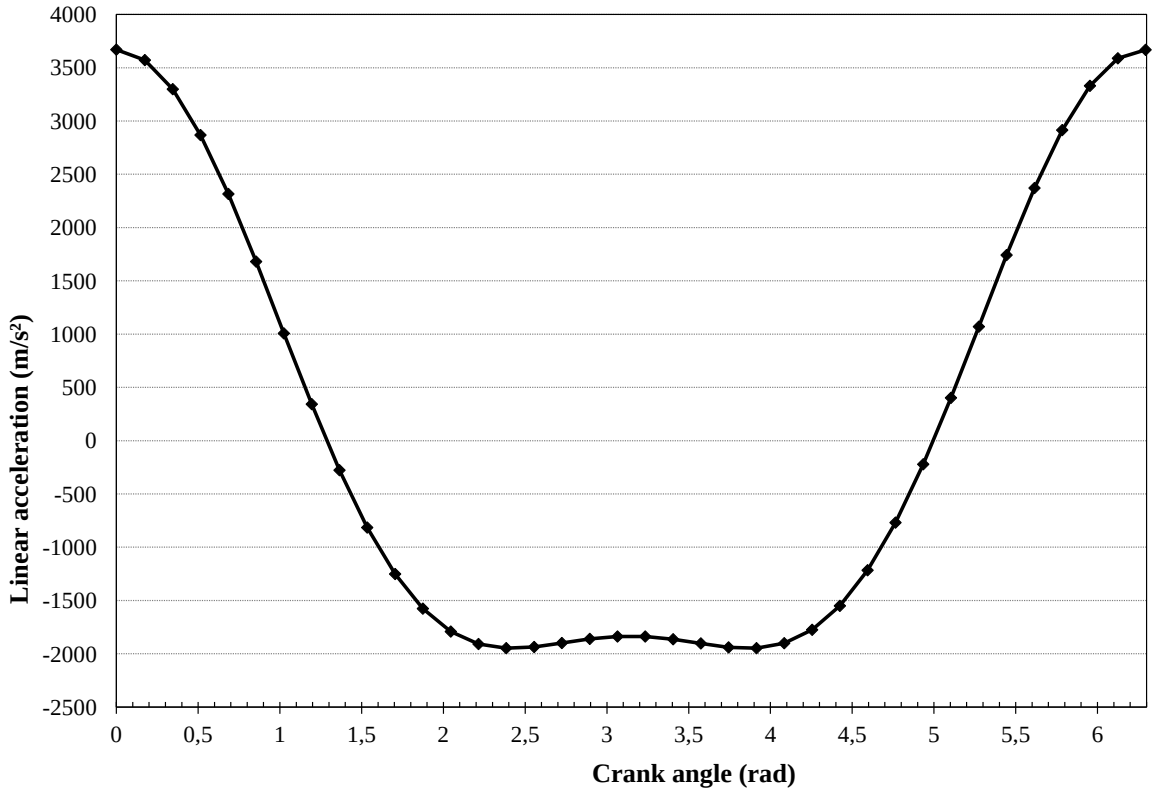

Figure 3.6 Linear acceleration graphic

From the second law of Newton, it is possible to calculate the inertia on the piston. The linear acceleration is multiply by a scalar.

$$F = m * a \tag{3.9}$$

Where,

$$m = m_{piston} + m_{rod} \tag{3.10}$$

The piston mass is 2.379 kg and the rod mass is 4.110 kg, the maximum of inertia force is reached os TDC positon, the value is 23886 N.

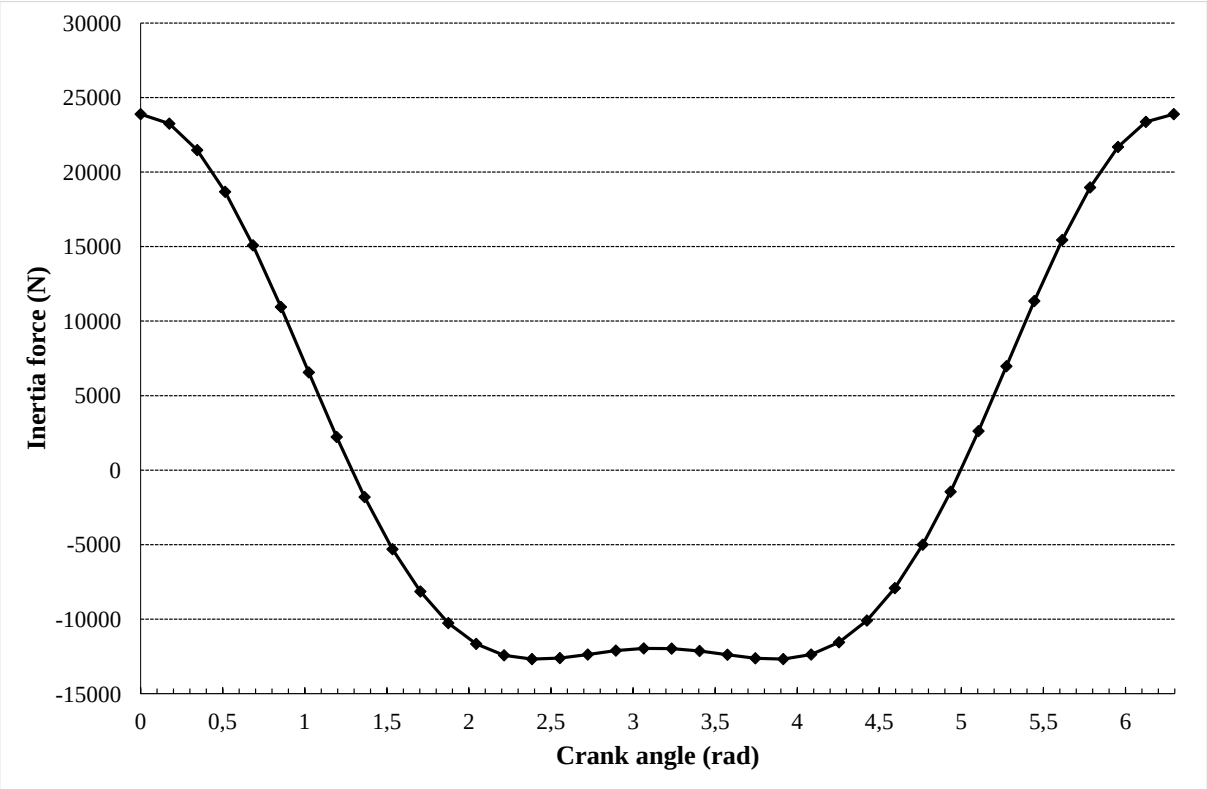

Figure 3.7 Inertia graphic- conventional piston

3.3 Static analysis-conventional piston

The Figure 3.8 shows the main three steps of the simulation. The first one is the material input, the material properties are directly applied to the CAD model. The second step is to create a mesh on the piston. The mesh has to be small enough to cover all the geometries and represents them properly. The final step is to run the analysis, with the main inputs and analyse the results.

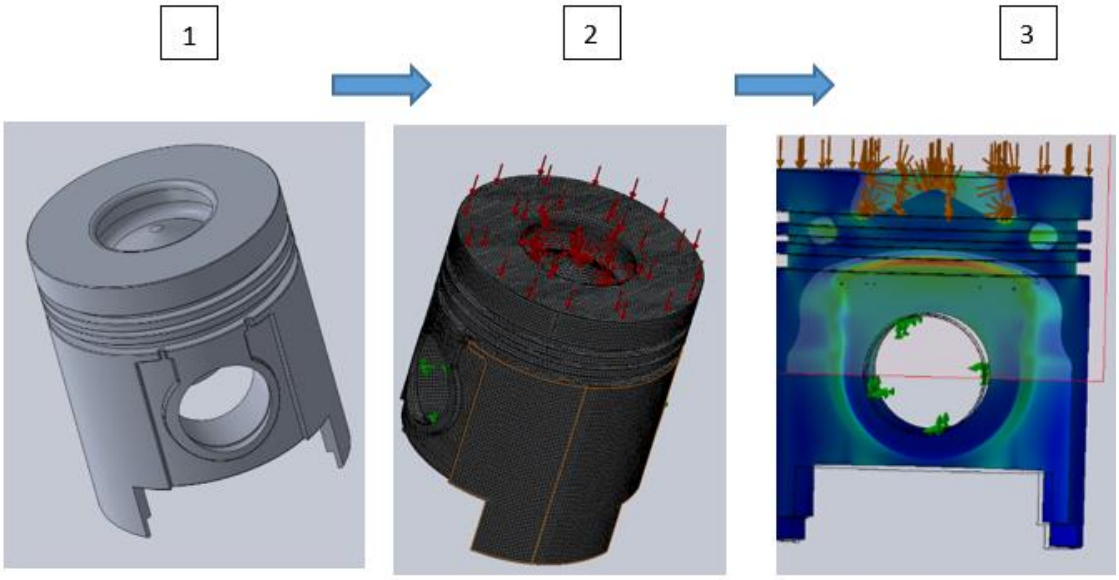

Figure 3.8 Simulation steps

The chosen material on the simulation was an aluminium alloy with surface treatment, 4032 T6. On the two next tables mechanical properties and the percentage of the elements are shown, Table 3.3Table 3.4. [17]

Table 3.3 Mechanical properties of the aluminium alloy 4032 T6

Properties	Value
Tensile strength in X (MPa)	380
Yield strength (MPa)	315
Young's modulus, E (GPa)	70-80
Poisson ratio	0.33
Density(g/cm^3)	2.69

Table 3.4 Contents of the aluminium alloy 4032 T6

Element	Content (%)
Aluminium, Al	remainder
Silicon, Si	12.5
Magnesium, Mg	1.0
Copper, Cu	0.9
Nickel, Ni	0.9

Static analysis is used to calculate how a certain component reacts to some giver conditions, load configurations. For accurate results on complex components, a computer program that uses the Finite Element Method (FEM) is very convenient.

For structural analysis, three steps allows the formation, results and analysis of a computer model of the piston.

Given a meshed model with a set of displacement restraints and loads, the linear static analysis program proceeds as follows: [18]

- The program constructs and solves a system of linear simultaneous finite element equilibrium equations to calculate displacement components at each node.
- The program then uses the displacement results to calculate the strain components.
- The program uses the strain results and the stress-strain relationships to calculate the stresses.

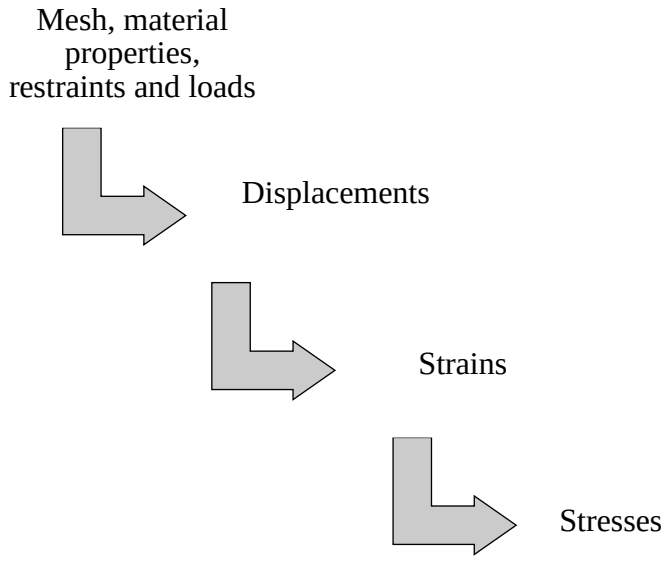

Figure 3.9 Static analysis process [18]

In this study, numerical results were obtained using a finite elements software, SolidWorks™.

The first step is to define boundary conditions, in this case the piston is tested during the expansion of the gases on the TDC position. The simulation is done in SolidWorks™ only takes into account the gas pressure applied on the piston crown, 18 MPa, from the state of the art,

Table 2.1.The pressure is applied normal to the surface, see Figure 3.10. The results obtained from the simulation will show how the tensions spread on the piston.

Piston pin hole is constrained by displacement and symmetry, fixed feature, this restraint type sets all translational degrees of freedom to zero.

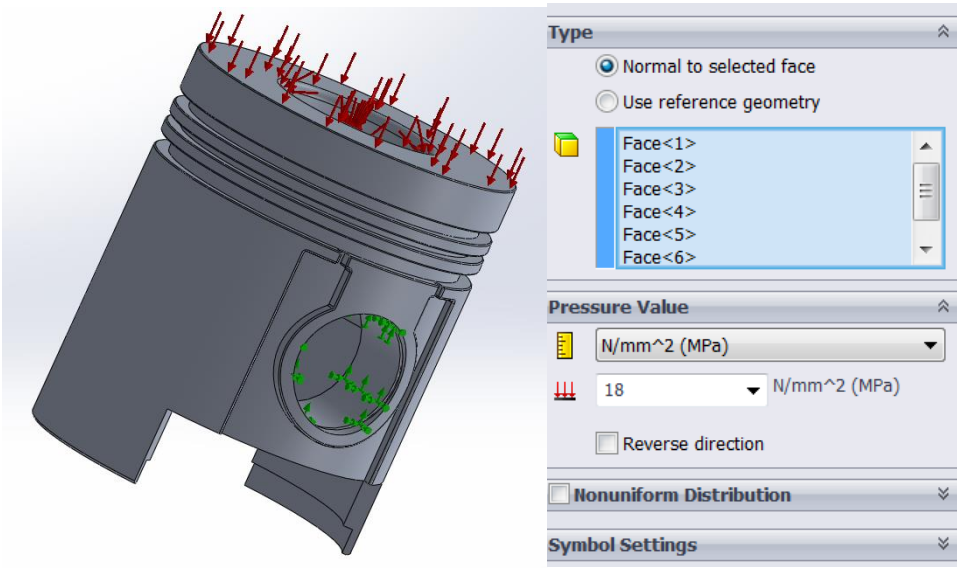

Figure 3.10 Constraint feature- conventional piston

3.3.1 Mesh

In meshing a part or an assembly with solid elements, the software generates one of the following types of elements based on the active mesh options for the study:

- Draft quality mesh. The automatic mesher generates linear tetrahedral solid elements.
- High quality mesh. The automatic mesher generates parabolic tetrahedral solid elements.

Linear elements are also called first-order, or lower-order elements. Parabolic elements are also called second-order, or higher-order elements.

A linear tetrahedral element is defined by four corner nodes connected by six straight edges. A parabolic tetrahedral element is defined by four corner nodes, six mid-side nodes, and six edges. [18]

The Figure 3.11shows schematic drawings of linear and parabolic tetrahedral solid elements.

In general, for the same mesh density (number of elements), parabolic elements yield better results than linear elements because:

- They represent curved boundaries more accurately, and
- They produce better mathematical approximations. However, parabolic elements require greater computational resources than linear elements.

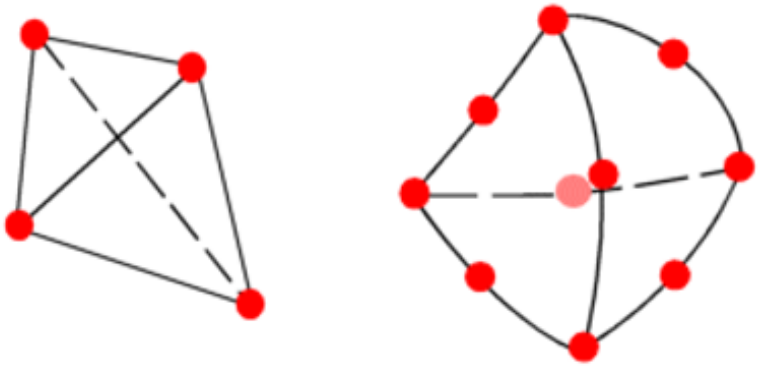

Figure 3.11 Types of Solid mesh [20]

For structural problems, each node in a solid element has three degrees of freedom that represent the translations in three orthogonal directions. The software uses the X, Y, and Z directions of the global Cartesian coordinate system in formulating the problem.[19]

In Figure 3.12 presents some of the mesh details used on the static study, the percentage of cells with aspect ratio lower than 3 is 99%, which means the ratio between the longest and the shortest side of the cells is 3 or less, ideally this ratio should be near 1 to ensure better results.[20]

Mesh Details

Study name	Study 3 (-Default-)
Mesh type	Solid Mesh
Mesher Used	Standard mesh
Automatic Transition	Off
Include Mesh Auto Loops	Off
Jacobian points	4 points
Element size	1.7702 mm
Tolerance	0.0885101 mm
Mesh quality	High
Total nodes	1130177
Total elements	752361
Maximum Aspect Ratio	26.931
Percentage of elements with Aspect Ratio < 3	99.3
Percentage of elements with Aspect Ratio > 10	0.00106
% of distorted elements (Jacobian)	0
Time to complete mesh(hh:mm:ss)	00:03:58
Computer name	

Figure 3.12 Mesh details

3.3.2 Maximum von Mises Stress Criterion

The maximum von Mises stress criterion is based on the von Mises-Hencky theory, also known as the shear-energy theory or the maximum distortion energy theory.

In terms of the principal stresses σ_1, σ_2, σ_3, the von Mises stress is expressed as:

$$\sigma_{vonMises} = \sqrt{[(\sigma_1 - \sigma_2)^2 + ((\sigma_2 - \sigma_3)^2 + (\sigma_1 - \sigma_2)] \cdot \frac{1}{2}} \tag{3.11}$$

The theory states that a ductile material starts to yield at a location when the von Mises stress becomes equal to the stress limit. In most cases, the yield strength is used as the stress limit. However, the software allows you to use the ultimate tensile or set your own stress limit.

$$\sigma_{vonMises} \geq \sigma_{limit} \tag{3.12}$$

Yield strength is a temperature-dependent property. This specified value of the yield strength should consider the temperature of the component. The factor of safety at a location is calculated from: [21]

$$\text{Factor of Safety (FOS)} = \sigma_{limit}/\sigma_{vonMises} \quad (3.13)$$

3.3.3 Stress results- Gas pressure

The following figure, Figure 3.13, shows the simulation results. As it is possible to understand the highest stress load is around 182 MPa, which is under the yield strength of the material (315 MPa). This value will be the reference to the design optimisation, which means that the maximum stress of the optimised piston cannot be greater than the maximum stress of the conventional design, around 182 MPa.

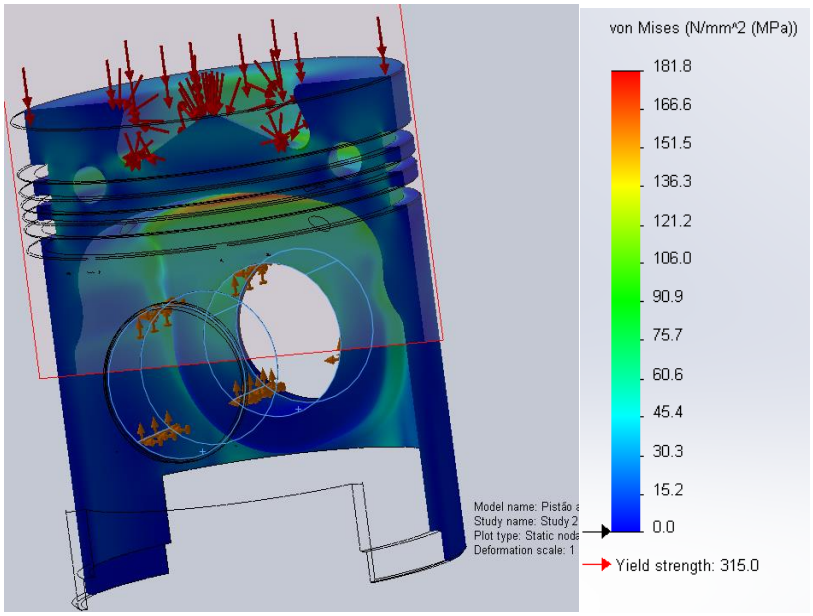

Figure 3.13 Static analysis- conventional piston

As it is possible to observe, in Figure 3.14, the maximum stress appears on the top of the piston boss, between the transition of the piston crown and the main body of the component, where the geometry loses its continuity that is why stress risers happened. Those areas are called critical areas.

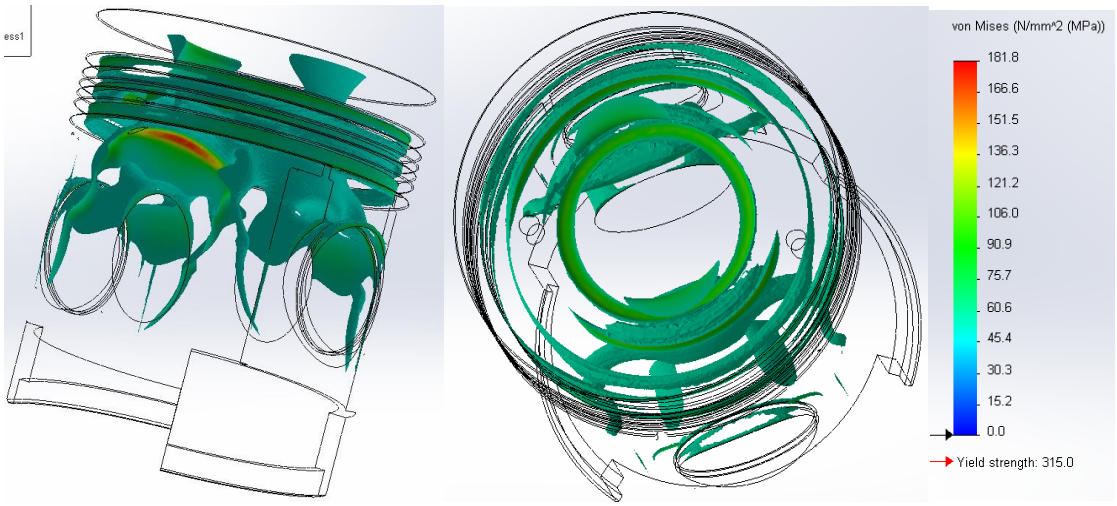

Figure 3.14 Maximum stress of the static analysis- conventional piston

The Figure 3.15 shows a different plot of these simulation, the displacement over the piston. As it is shown on Figure 3.15, the maximum displacement occurs on the lower part of the piston, due to the input of the constraints on the simulation. The piston body and the pin boss are fixed. The maximum displacement is 8.270×10^{-2} mm, and in placed on the piston skirt and on the top of the piston. The maximum displacement are placed on the opposite direction of the pin bosses due to the fixed feature. The displacement is bigger on the lower part of the skirt because of its thickness, the lower part is thinner than the upper part.

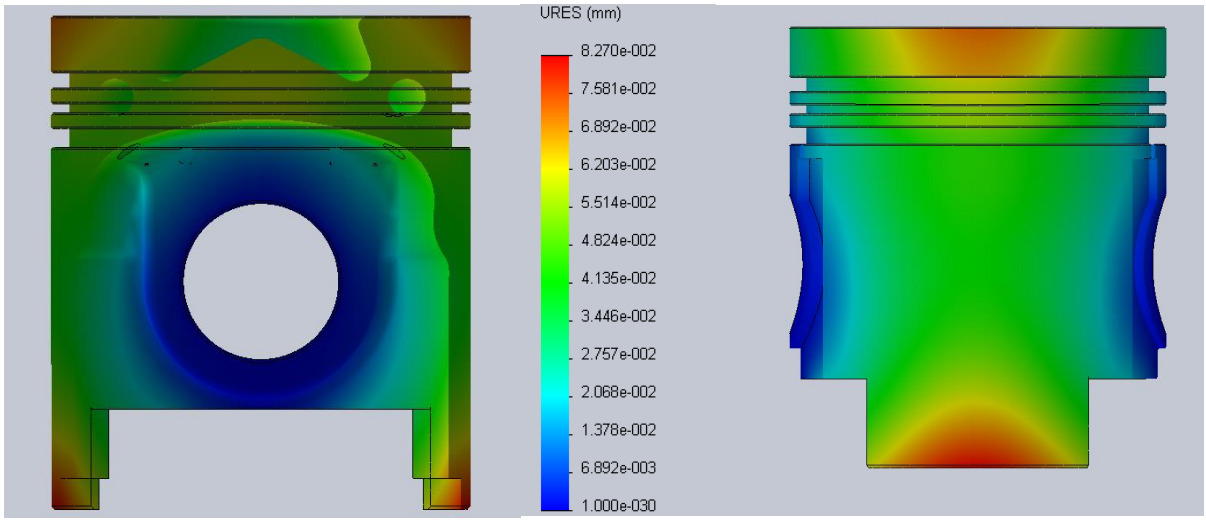

Figure 3.15 Displacement results- conventional piston

The Figure 3.16 shows the factor of safety among the piston. This factor is a relationship between the yield strength and the results from each location, see section 3.3.2. As it was

expected the factor is always greater than 1, as it was present on the static results the highest stress is about 1.7 times lower than the yield strength and it is represented by the factor of safety. The lower factor is placed where the stresses are greater and the other way around is true.

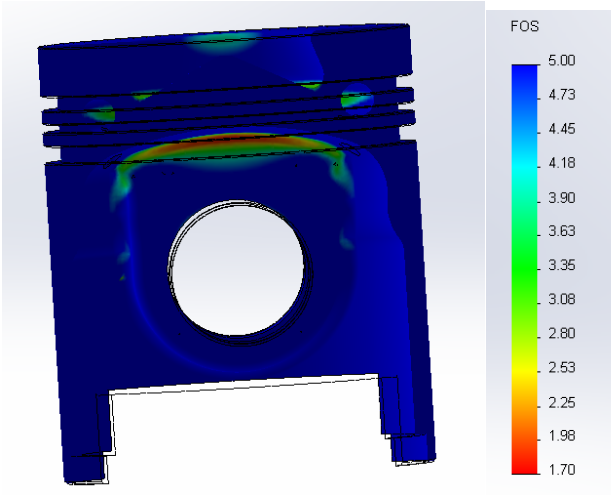

Figure 3.16 Factor of safety- conventional piston

3.3.4 Static analysis results- Inertia

The inertia was computed through the acceleration results, see Figure 3.7. The highest value was the input of this simulation, the results are present in Figure 3.17. The maximum stress is located on the outside of the piston boss, 171 MPa. The force, which was calculated on the section 3.2, is applied on the pin boss.

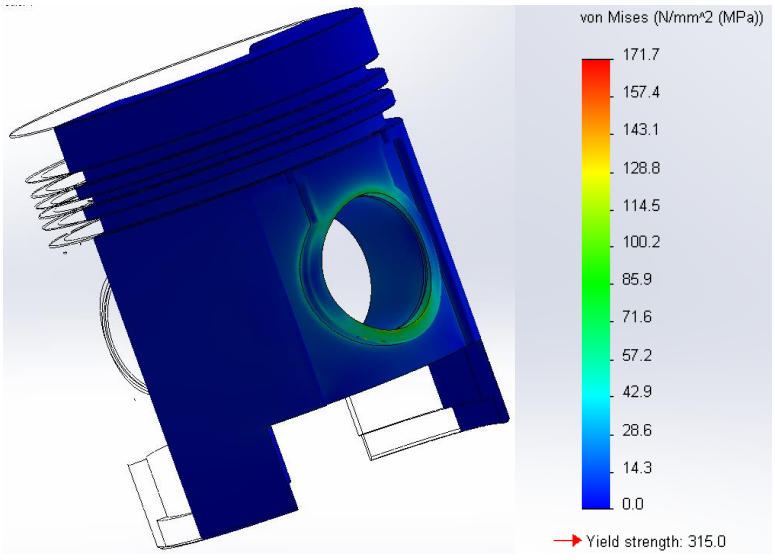

Figure 3.17 Inertia- conventional piston

3.4 Thermal analysis

When simulating operation conditions of a piston, it is important to compute the heat transfer between the walls of the piston to the cylinder and the heat transfer to the combustion chamber. It is important to perform a thermal analysis on the piston in order to track and control the thermal stresses and deformations.

The thermal analysis of the piston is important from different points of views. First, the highest of any point should not exceed 66% of the melting point temperature of the alloy 4032 T6, between 532 and 571ºC. [22]

A thermal analysis of the piston was performed. The thermal boundary conditions have been applied to the 3D model. Temperature distribution of piston was obtained using four different boundary conditions:

- Heat transferred from the combustion gases to the piston crown;
- Heat transferred to the engine oil from the outside of the piston;
- Heat transferred to the engine oil from the underside of the piston;
- Heat transferred form the cooling gallery to the oil.

The next table shows the main properties of the oil 15W40, a typical oil used on heavy duty engines. Those properties were used the compute the heat transfer coefficient all the inputs between the wall of the cylinder and the piston.[23]

Table 3.5 oil properties

Oil properties, 15W40	
Specific heat Cp	2.19 kJ/kgK
Thermal conductivity k	0.137 W/mK
Kinetic viscosity γ	14.1×10^{-6} m^2/s

The Table 3.6 shows the main properties of the impinging jet. Those properties were used to compute the heat transfer coefficient the oil the remains the inside of the piston cooled and the underside of the piston.[23]

Table 3.6 Jet properties

Jet properties	
Diameter	2.2×10^{-3} m
Velocity$_{jet}$	20 m/s

The piston used for the present simulation is a piston from heavy duty transportations and the follow table, Table 3.7, presents its main data for the simulation.

Table 3.7 Piston information

Piston data	
Length	158×10^{-3} m
v_{med}	9 m/s

3.4.1 Boundary conditions

It considers that a heat transfer between the cylinder wall and the piston is similar as in between two parallels plates, see Figure 3.18.[24] The conduction coefficient was computed with equation 3.14.

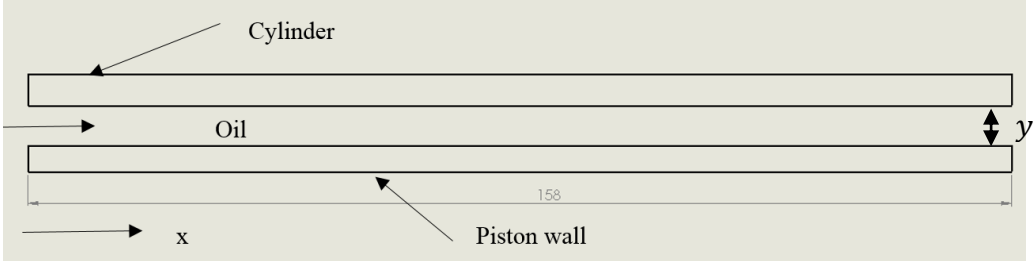

Figure 3.18 Scheme of the heat transfer between the cylinder and the piston wall

$$h = \frac{k}{y} \tag{3.14}$$

Where y is the oil thickness, see Figure 3.18 , which is $70 \times 10^{-6} m$.

The software does not allow a conduction input, so the value obtained was insert as a convection coefficient.

The second input is related to the cooling system. The convection coefficient of the inner side is computed trough a system of jet impingement, demonstrated on Figure 3.19. Basically, the oil injector troughs oil to the inner surface of the system. The calculations were made with a z_0 constant as well as the velocity of the piston.

The piston is cooled in two different ways. Part of the heat is driven through the segments to the liner and finally to the coolant. The greater part, though, is transferred to the oil. In the

engine under normal operating conditions the oil. With the temperature of 120℃, is sprayed to the inner part of the piston, see Figure 3.19. A numerical model was developed using finite element methods for studying the oil jet cooling of the piston. The jet, diameter on this study, is 2.2 mm on Table 3.8.

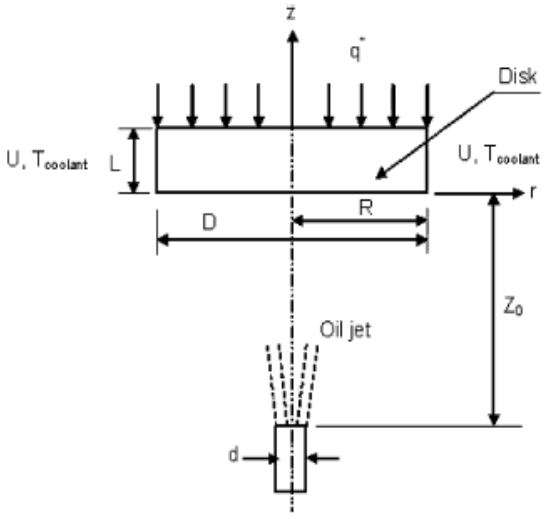

Figure 3.19 The coordinate system used for the notations for oil jet cooling [23]

$$\frac{Nu}{Nu_0} = \left[1 + f\left(\frac{r}{d}\right)^{-9}\right]^{0.11} \tag{3.15}$$

$$f\left(\frac{r}{d}\right) = ae^{b(\frac{r}{d})} \tag{3.16}$$

$$Re = \frac{\rho Ux}{\mu} = \frac{Ul}{\gamma} \tag{3.17}$$

$$Nu_0 = 2.67Re^{0.567}Pr^{0.4}(\frac{z0}{d})^{-0.336}(\frac{v}{d})^{-0.237} \tag{3.18}$$

$$v = v_{jet} - v_{piston} \tag{3.19}$$

Table 3.8 Values of a and b [23]

d [mm]	a	b
2.2	1.13	-0.23
2.3	1.141	-0.2395
4.1	1.34	-0.41
5.8	1.48	-0.56
8.9	1.57	-0.7

On the combustion chamber the heat transfer was compute trough the equation (3.20). [12]

$$h = 3.26p^{0.8}v^{0.75}D^{-0.2}T^{-0.465} \tag{3.20}$$

The pressure is the gas pressure, 18 MPa and the velocity is the piston average velocity which is 9 m/s. TheTable 3.9, shows the different values of heat convection coefficient, since the velocity of the piston and the gas pressure is the same.

Table 3.9 Different values of h with fluctuations on the temperature

T(℃)	h (W/m^{2}k)
1500	167.67
1750	186.33
2000	204.54
2250	222.34
2500	239.80

Both of the thermal studies, either the conventional or the optimised piston, are made with the temperature of combustion of 1750℃. The other values will be studied, but only the maximum of temperatures will be present, the results will be present on the last section of this chapter.

3.4.2 Thermal analysis results- Conventional piston

The figure Figure 3.20 shows the thermal analysis results. As it possible to observe the highest temperature is located on the edge of the piston crown, 323℃. The temperature decreases on the ring belt and reaches the minimum, 120℃, on the skirt.

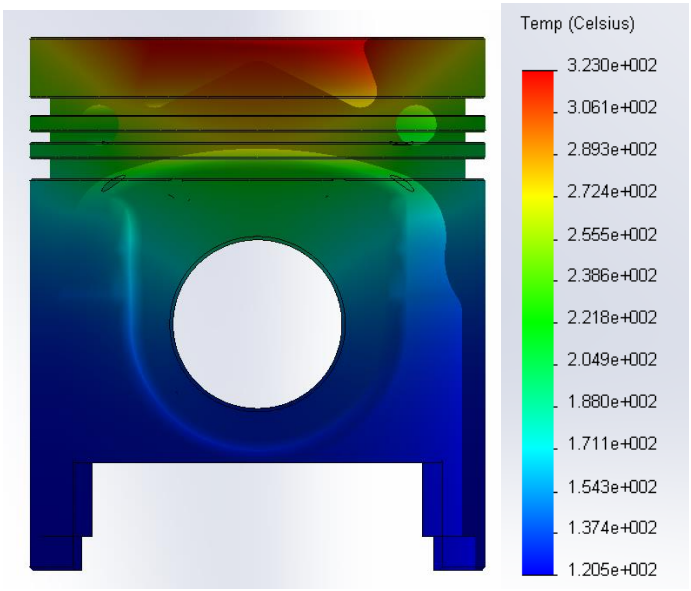

Figure 3.20 Temperature distribution in the piston- conventional piston

The Figure 3.21 represents a plot of the thermal analysis, where only a transversal cut of the piston is shown. This plot was performed in order to show the different temperatures on the piston ring zone. As we can see, the first ring reaches a, approximately, 240 ℃ then drops until 217 ℃ on the second ring, and the temperature of the third ring is around 198℃. So, we have a decrease of temperatures of the first to the second ring of 23 ℃ and the second to the third of 19℃, which means that the cooling gallery, placed between the first and the second ring, is cooling that region. Then, the temperature drops until 120 ℃ when reaches the skirt area.

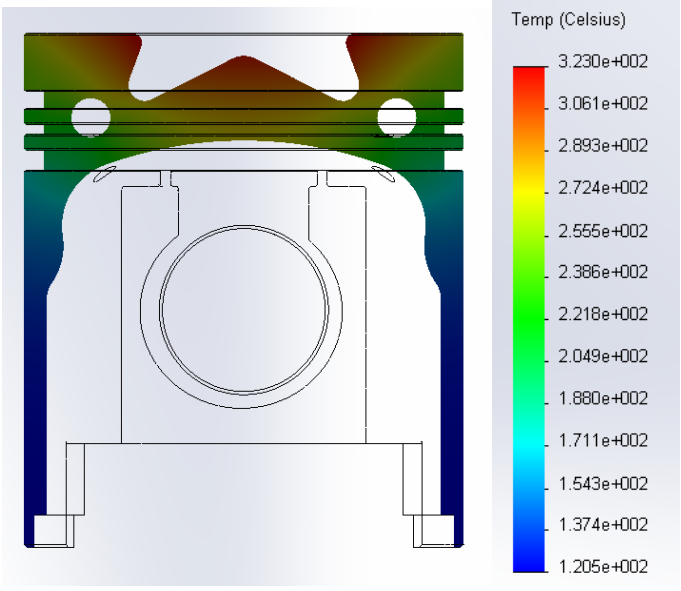

Figure 3.21 Thermal results section- conventional piston

In Figure 3.22 are present four sections of the top of the piston, this figure intends to show the difference of temperatures between the different layers of the top of the piston. The temperature is becoming lower and lower on the XX axis. On the top of the piston the highest temperature is 323 ℃ as it was said before, and the lowest temperature is 268℃. On the second section, 10 mm from the top, the average of temperatures decreases the highest temperature is 305℃ and the lowest is 250℃. The third section, 20 mm from the crown, the highest temperature is around 290℃ and the lowest is 260℃. The final section, where is placed the gallery, shows that the highest temperature is 276℃ in the centre but in the periphery the temperature is approximately 242℃.

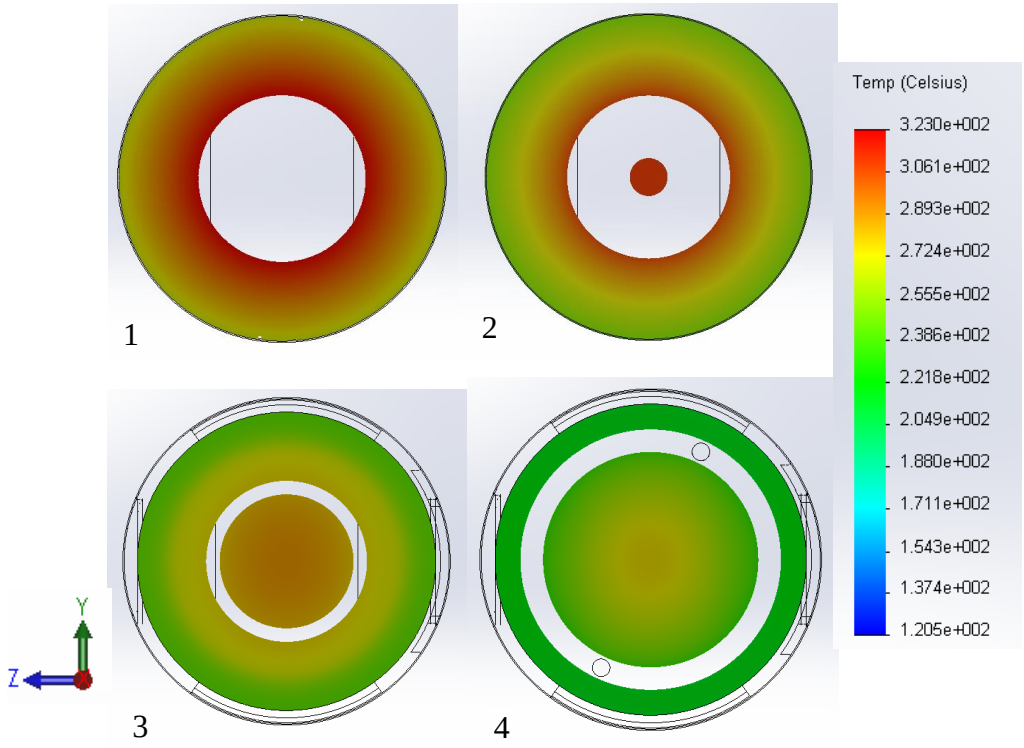

Figure 3.22 Sections views of the crown (1-0mm from the top, 2- 10 mm from the top, 3- 20mm from the top, 4-20 mm from the top-conventional piston)

The next two figures are the temperatures distribution on the piston crown, Figure 3.23, and the wall, Figure 3.24. The highest temperature is on the edge of the piston crown, which is agreeable with the state of the art, see Figure 2.7. The profile of temperatures on the wall, Figure 3.24, is similar to the state of the art profile, the temperature decreases as the distance between the top of the piston and the bottom becomes greater. However the profile of the temperatures present on the piston crown shows an increase of temperature on the centre, although the maximum of temperature is agreeable with Figure 2.7, which is between 270 and 380℃.

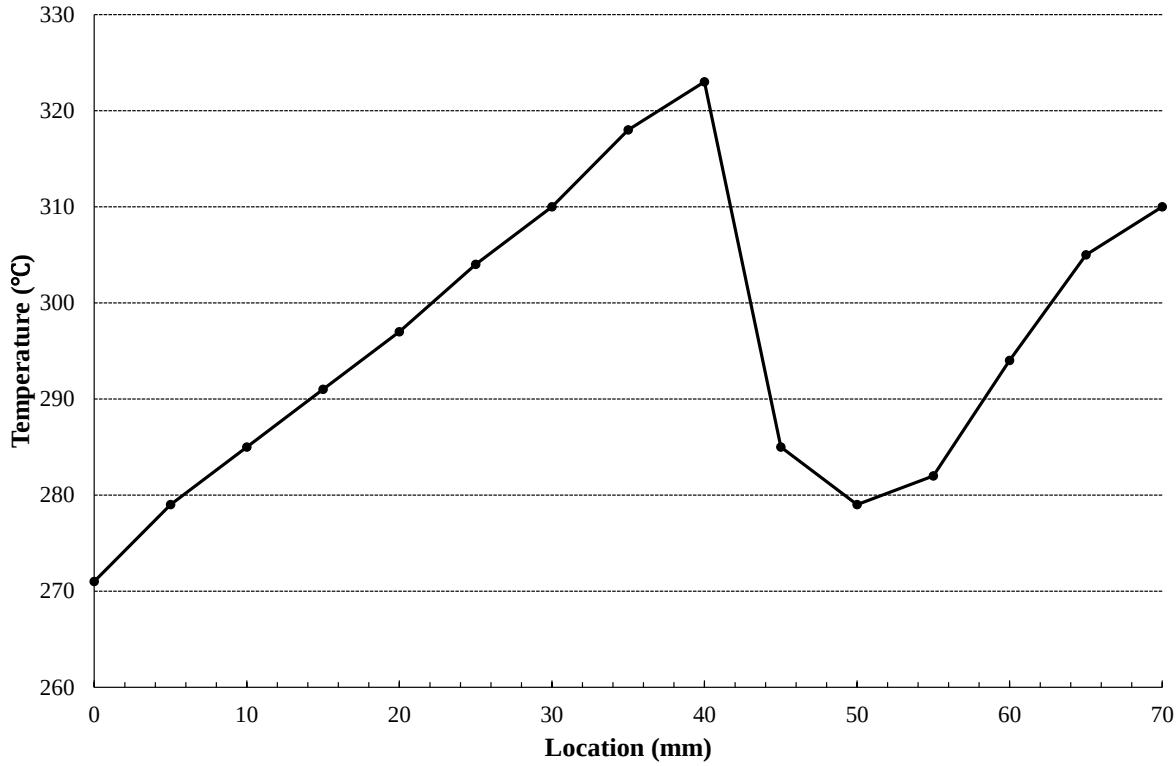

Figure 3.23 Profile temperatures crown

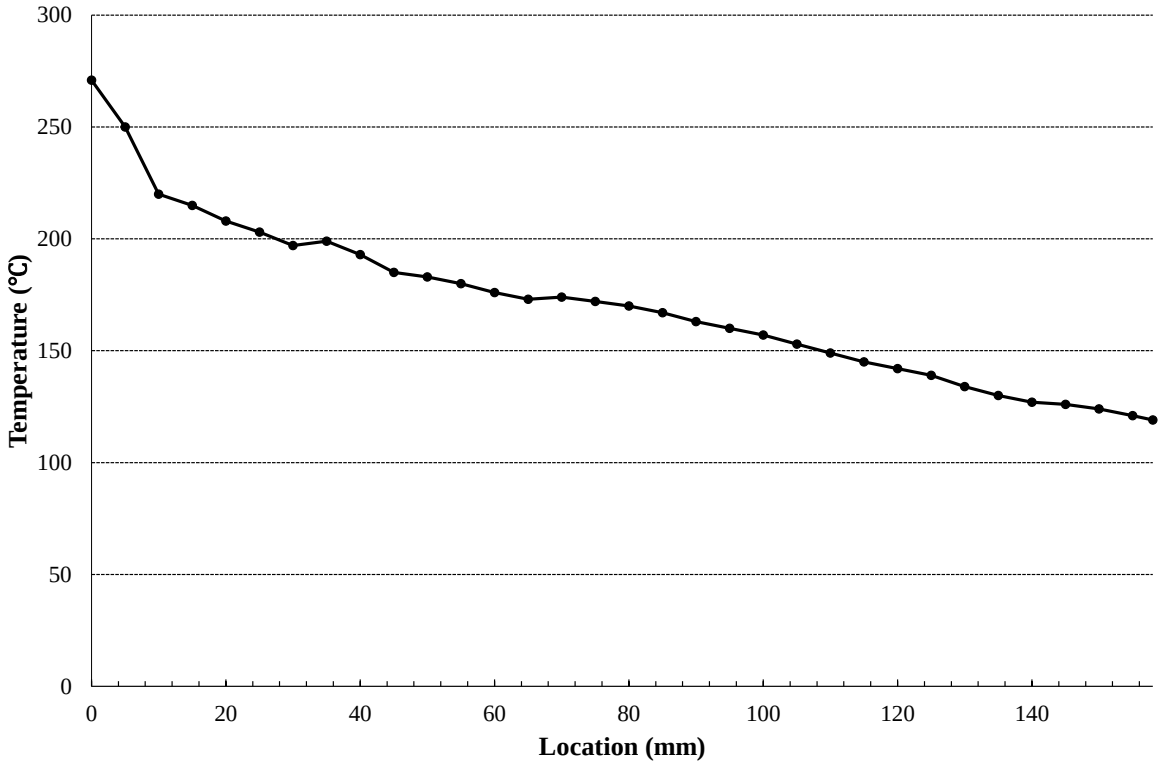

Figure 3.24 Profile temperatures wall

In Figure 3.25 is presented a heat flux plot of the thermal analysis. It is possible to verify that the highest heat is transferred trough the piston gallery. Those results were expected, since the gallery has that function, cool the top part of the piston. Besides the gallery, the third piston ring region also shows a large heat flux. The highest value of heat flux is $7 \times 10^5 W/m^2$.

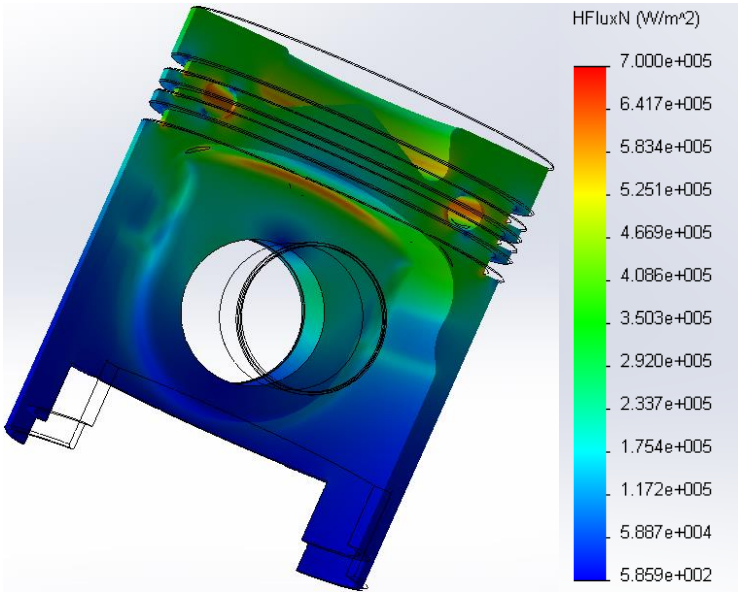

Figure 3.25 Heat flux in the piston- conventional piston

3.5 Optimisation

The final goal is to reduce 30% of the mass of the piston using a cellular structure capable to support the gas pressure and at the same time dissipate the heat from the combustion.
In order to make the whole process easier a mass sensor, see Figure 3.26, was added during the development of the new piston. The sensor appears in the Constraint sect of the software.

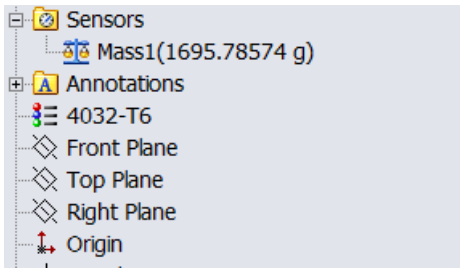

Figure 3.26 Mass sensor

The majority of the piston mass is located in the area from the centre of the piston to the edge of the piston crown, making those regions a target of the optimisation.

3.5.1 Main body

The first step was, by applying the basis of cellular structures, to make the walls as thinner as possible, creating a skin. Once simulating with different thicknesses, 4 millimetres was the lowest value with this kind of restrictions, see Figure 3.27. On the skirt zone a thickness is 2.75 mm. The command used was shell, where is possible to define how width of the wall.

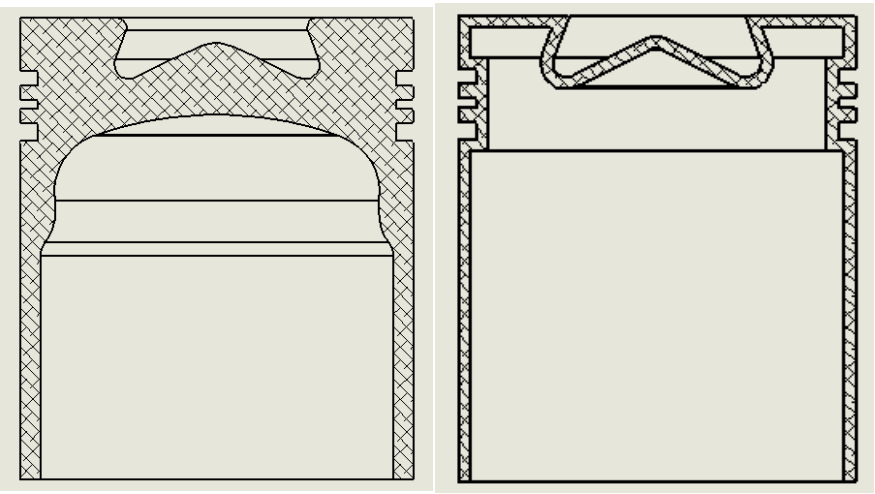

Figure 3.27 Wall thickness- optimised piston

In order to keep the same stress flow the same curvature was used, spotted in red, the reason why there is a bulk of mass around all the piston, see Figure 3.28. On the left is present a section of the conventional piston and on the right is the optimised piston.

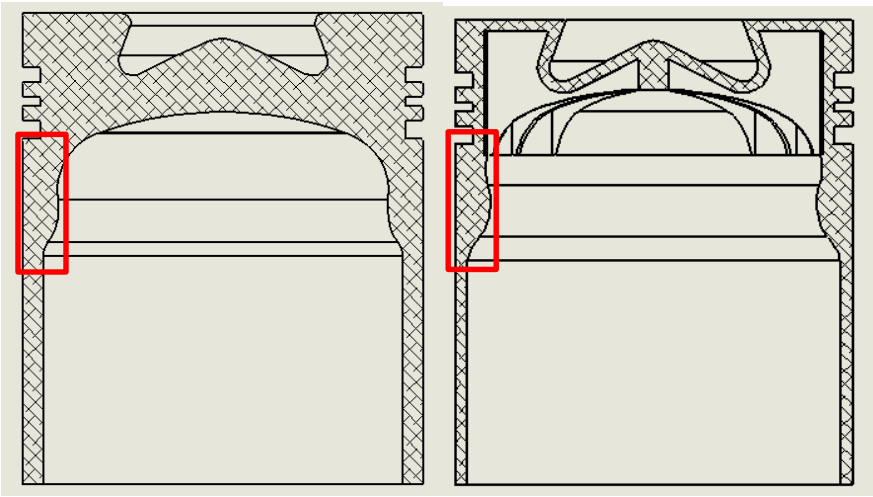

Figure 3.28 Inner side curvature

The conventional piston has a thickness of 7mm on the lower part and the mass of the body, without the cooling gallery and the pin boss, is 2.367 kg the mass of the optimised body of the piston, without the ribs on the piston crown, is 1.267 kg. Which makes the body of the new piston 46% lower than the conventional piston.

3.5.2 Crown

A weight optimisation was performed on the piston. In Figure 3.29 it is possible to observe the new piston crown. This new crown is built with eight ribs, two millimetres each one, and two large bulks of material on the upper part of the pin boss due to high stresses, verify on the static analysis of the conventional piston.

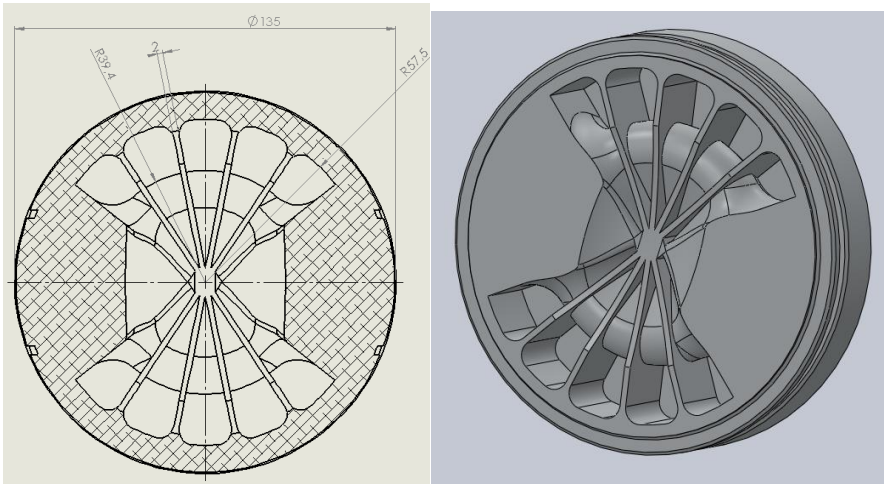

Figure 3.29 Piston crown measurements and 3D model- optimised piston

The design of the crown was thought this way to make sure that the heat can be dissipated trough the ribs due to the total removal of the cooling gallery, so the area of the new inner crown is 32350mm^2, 3.4 times greater than the conventional inner crown with the gallery.

3.5.3 Piston boss

After understanding how the stresses develop over the body is, and because there were only two boundary conditions, the gas pressure on the crown and the inertia on the pin boss, the higher stresses were situated on the upper part of the piston making the lower part less stressed which results on removing material on the lower part. At first a cellular structure was apply to the lower part of the pin boss, see Figure 3.30, however due to the complexity of the geometry was not possible to performed a static analysis on it.

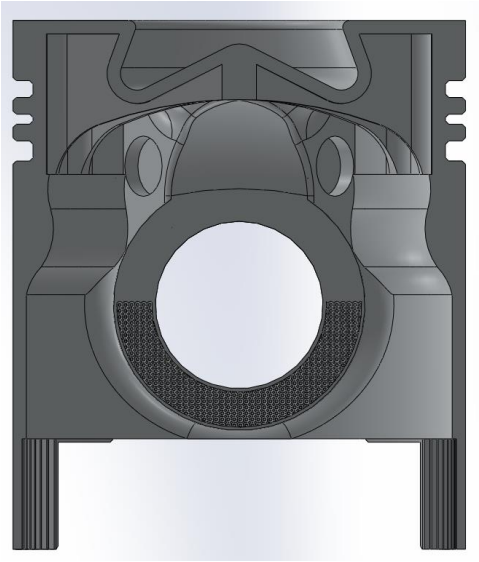

Figure 3.30 Pin boss with a cellular structure

The cellular structure applied is made by an open-cell with 1mm of radius repeated on X, Y and Z direction. [3] Every two spheres intersect with each other generating a thin wall, see Figure 3.31. The thickness around the pin boss is 1mm.

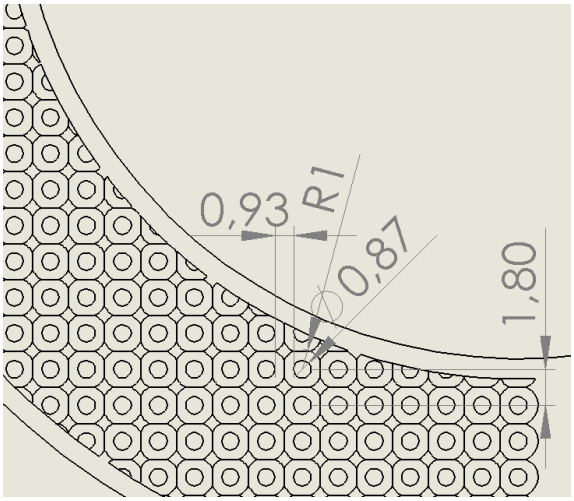

Figure 3.31 Cellular structure

The problem of this type of this cellular structure is that is built on the 3 axis direction, which is not flawless on the connection between the cellular structure and the wall around the pin boss, see Figure 3.32. It is possible to verify that the connection is no perfect, leaving same areas with more contact and another areas with less contact, which can lead to different stresses, considering the contact area between the wall and the cellular structure.

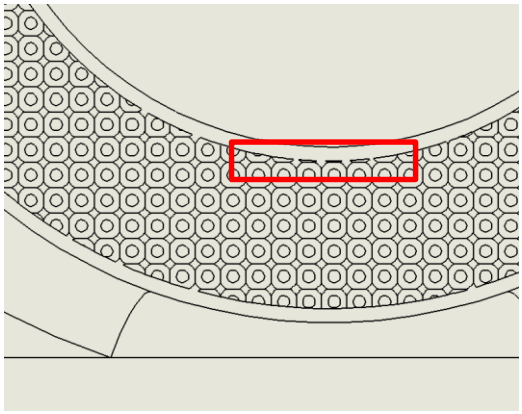

Figure 3.32 Connection between the cellular structure and the wall

After the design with the cellular structure another solution was created. The material is placed more on the upper part leaving the lower part with a thickness of 2 mm and ribs with 2 mm as well, see Figure 3.33.

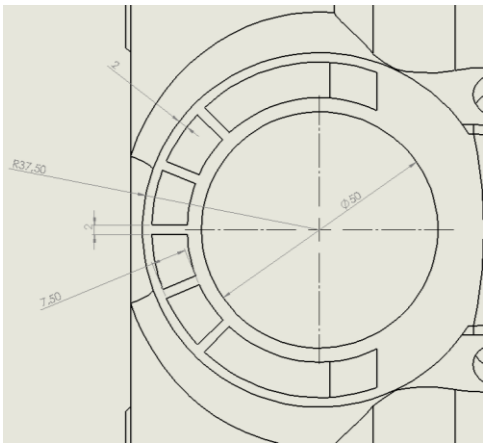

Figure 3.33 Piston section- optimised piston

3.5.4 Skirt

The lateral forces were not tested, so the main changes on the skirt were its thickness and fins were added around the inner part of the skirt to help the heat dissipation. There are 34 fins around the skirt, each of them as a width of 1 mm and a height of 2mm. The thickness of the skirt wall is 0.75 mm, see Figure 3.34. The conventional skirt has a thickness of 3mm.

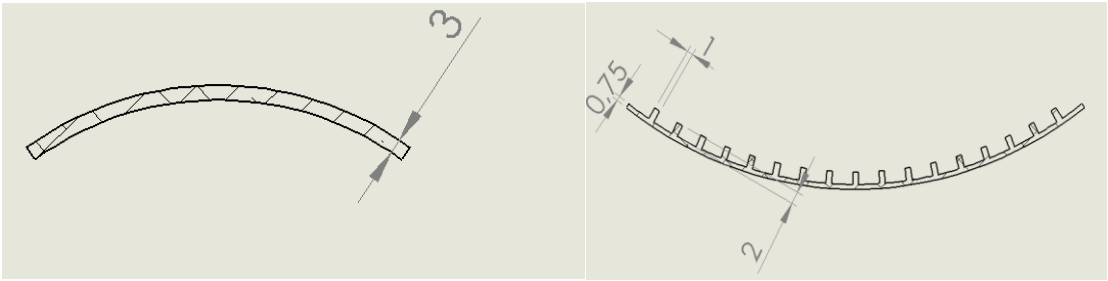

Figure 3.34 Section view of the skirt, on the right of the conventional piston and on the left of the optimised piston

The Table 3.10, presents the volumetric properties after the process. The mass of the new piston is around 1.696 kg.

Table 3.10 Volumetric properties, optimised piston

Volumetric properties	
Mass	1695.8 g
Volume	6.33×10^{-4} m^3
Surface Area	0.198 m^2

3.6 Static analysis – optimised piston

After the main changes on the piston design a static analysis was performed and the results will be presented on this section. As it is shown in Figure 3.35, the pressure, which is represented with the blue shifts, is the same as in the conventional piston, 182 MPa, which the same as in the conventional piston.

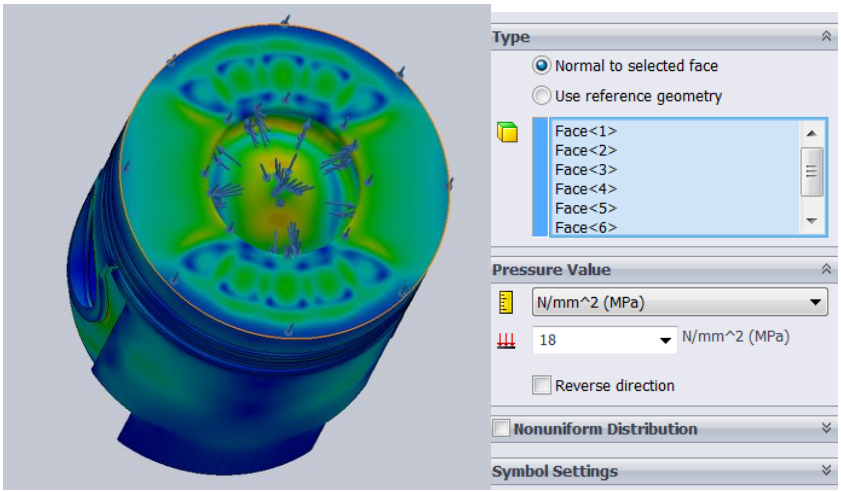

Figure 3.35 Static analysis results- optimised piston

The Figure 3.36 shows the results on the piston crown where it is possible to spot the stress risers are more spread than the conventional design, the red regions are not as dense as in the conventional static analysis. The stresses are shared on the piston crown, which gives a better distribution of the stresses. Moreover, the highest stress is placed in the same region as in the conventional piston, on the upper part of the piston boss.

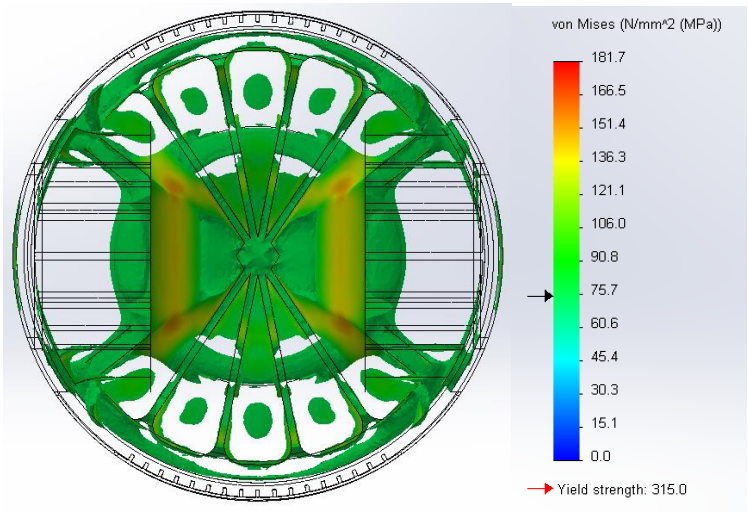

Figure 3.36 Static analysis results, probe above 75 MPa- optimised piston

The Figure 3.37 presents the factor of safety throughout the piston. This factor is greater the greater is the ratio between the tension of the location and the yield strength. As the tensions are the same as well as the material in both of the pistons the factor of safety is the same

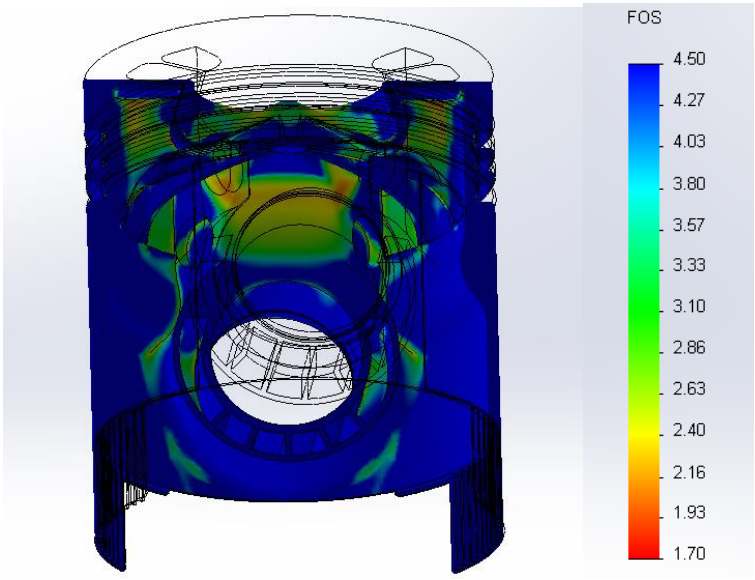

Figure 3.37 Factor of safety- optimised piston

The inertia was computed through the second newton's law, as in the conventional piston. The rod have the exact same mass as in the calculations of the inertia on the conventional piston, which means the connecting rod has the same mass 4.110 kg. The only difference is the mass of the piston, which is 1.695 kg. The results are present in Figure 3.38. The highest value of force is 21318 N, this will be the value to apply on the next simulation.

As in the linear acceleration and the inertia on the conventional pistons the lowest value is reached on BDC while the highest is attained on the TDC position.

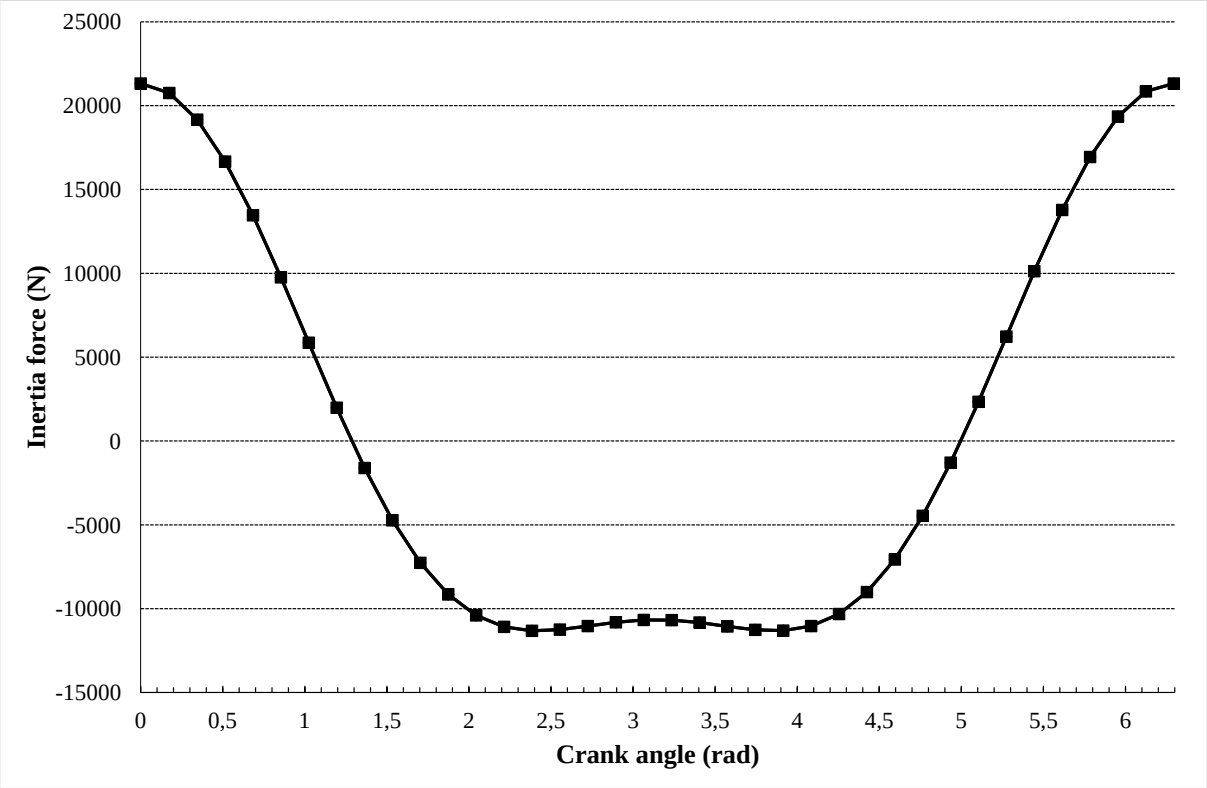

Figure 3.38 Inertia graphic- optimised piston

The Figure 3.39 presents the results of the static analysis, the force was placed on the pin boos feature and the rest of the body was considered fixed hinged which means that the piston it is allowed to slide on the X axis unlike the static analysis with the gas pressure where the body is

considered as a fixed component, as it is possible to observe the highest stress is on the outside and the down side of the pin boss. The highest stress obtained is 132.5 MPa.

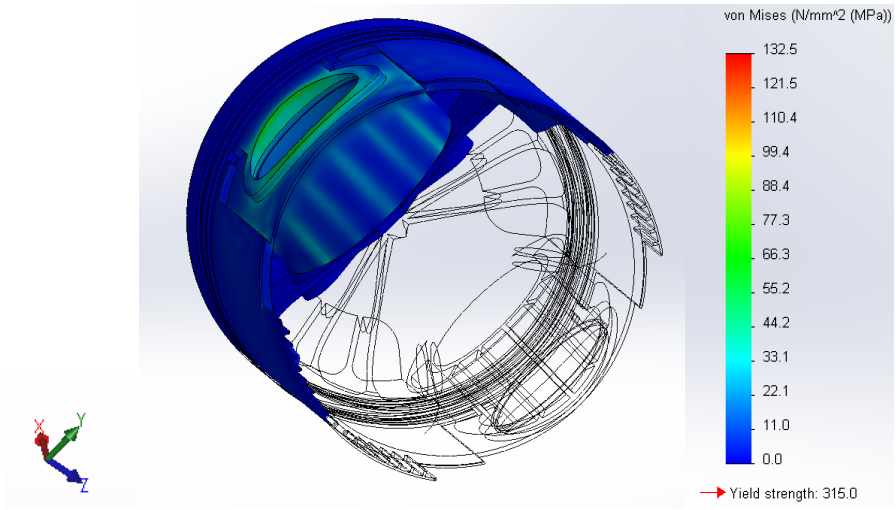

Figure 3.39 Inertia- optimised piston

3.7 Thermal analysis - optimised piston

The successful static analysis leads to a thermal analysis. The boundary conditions are the same of the conventional piston, the only difference is that this piston does not have a cooling gallery, so the convection coefficient is the same in all the inner side. The results are present in the Figure 3.40. The highest temperature is placed on the top of the piston, around 322℃, which is below than the conventional piston. There is a better dissipation of heat, which might mean that the oil is of the optimised piston is hotter than the oil of the conventional piston.

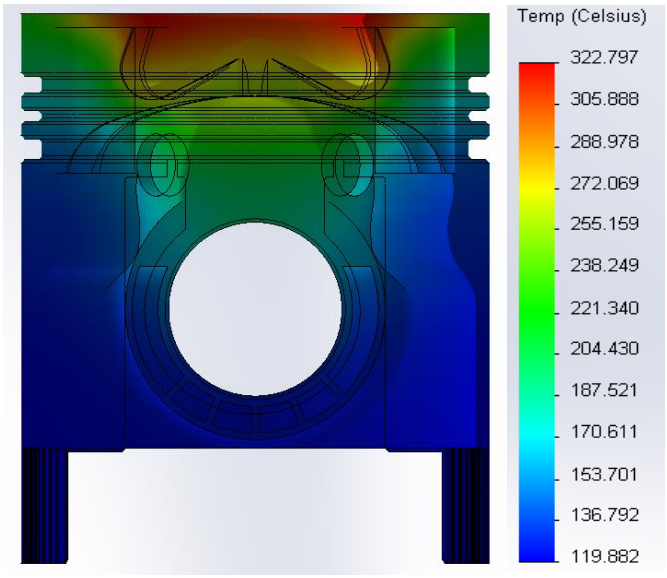

Figure 3.40 Thermal analysis results- optimised piston

The Figure 3.41 shows a section view on the plan XZ. This section was made in order to see the temperatures on the direction of the pin boss. As it is shown, on this direction, the first ring has a temperature around 226℃, the second ring reaches a temperature of 212 ℃ and finally the last ring score a temperature of 199℃.

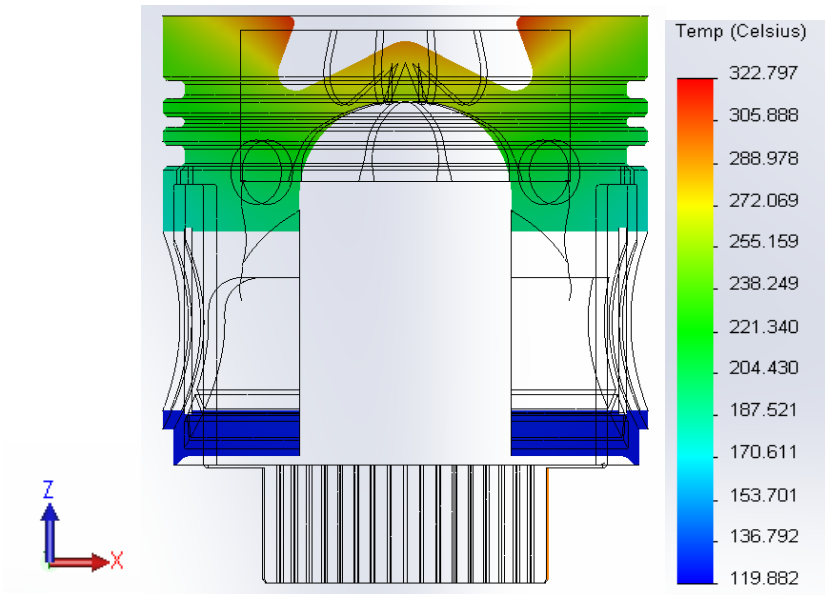

Figure 3.41 Section view, plan XZ

Due to the asymmetry of the piston, another section was needed in order to verify the temperatures values on the piston rings. As it is shown in Figure 3.42, the first ring as a

temperature value of 179℃ , the second ring the temperature is around 162 ℃ and the third ring reaches a temperature of 149℃ .

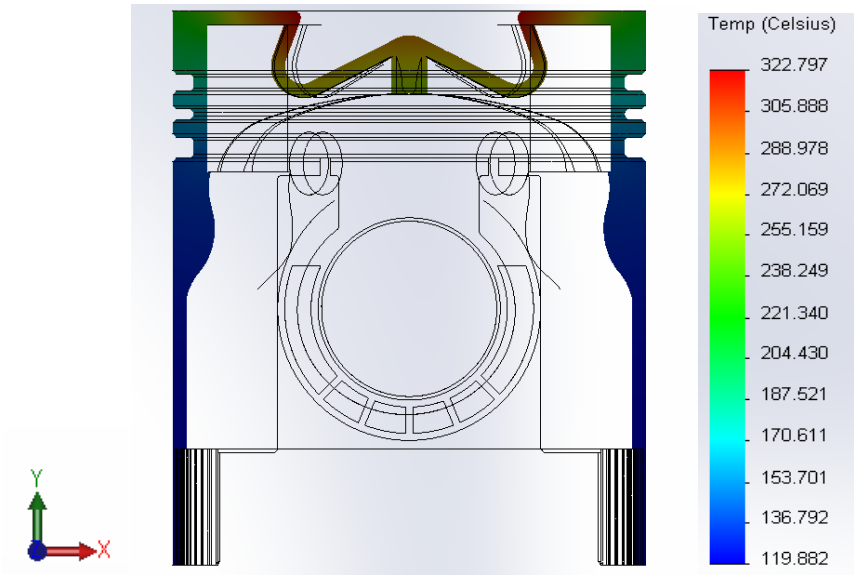

Figure 3.42 Section view, plan XY

It is known that the highest temperature is situated on the piston crown the Figure 3.43 shows a section view 10 mm bellow the top of the piston. As it is possible to see the temperature values are different depending on the location of the section, this is due to the different of thickness around the crown, Right on the top of the piston top, ZZ axis, the temperature is 235℃ on the periphery and on the interior is approximately 284℃. When the direction is changed, to YY axis, the highest temperature is 294℃ and the lowest temperature is around 202℃. It is possible to conclude that the decrease of the temperature on the ribs is greater than on the upper part of the pin boss.

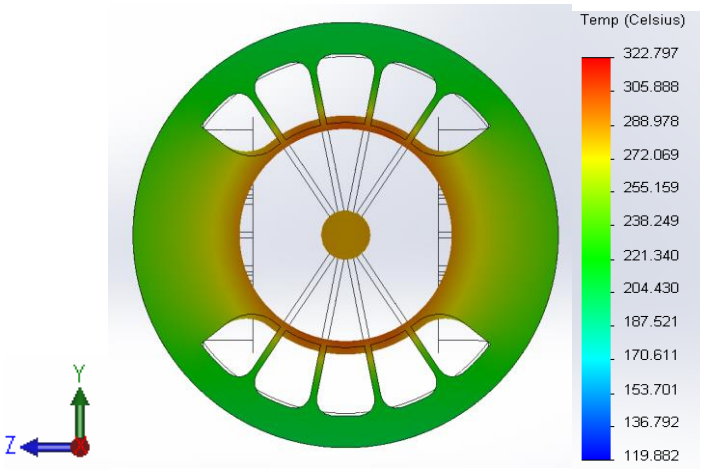

Figure 3.43 Section view 10 mm from the top- optimised piston

The Figure 3.44 shows the results of a plot of the thermal analysis, heat flux. The highest heat flux value is around$1 \times 10^6 W/m^2$. The oil is hotter on the inner side of the piston than on the piston walls, which means the fins on the piston crown are transferring the heat to the oil, as pretended. Although within the increase of oil temperatures the dynamic viscosity is lower, which means that the convection coefficient is lower.

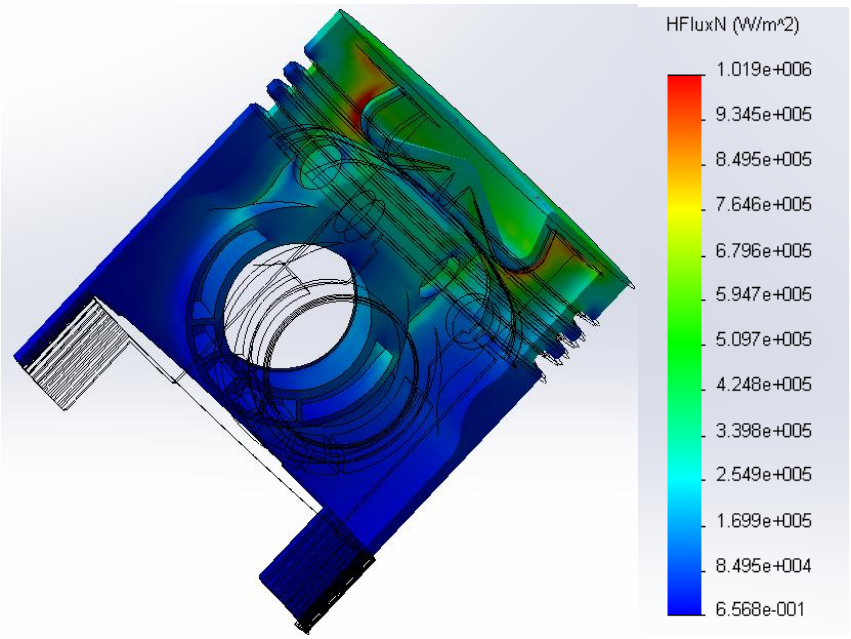

Figure 3.44 Heat flux- optimised piston

3.8 Results comparison

On Table 3.11 the results of both of the analysis, thermal and static, as well as the volumetric properties are present. As we can observe the mass was reduced is 29% and the maximum stress is essentially the same in both of the pistons. The surface area is 26% greater than the conventional piston, which helps the heat dissipation.

On the thermal analysis the results have shown that there is not a significant difference between the conventional piston and the optimised, the highest temperature achieved on the conventional piston was about 262 ℃ and the maximum obtained on the optimised piston was 258℃. However there is a significant difference between the heat fluxes, the heat flux achieved on the optimised piston is 48% higher than the conventional piston which can leads to a loss of thermal properties on the oil.

Table 3.11 Results

Results obtained	**Conventional Piston**	**Optimised Piston**		**Difference [%]**	
Volumetric Properties					
Mass	2379 g	1695.8 g		-29	
Volume	$8.88 \times 10^{-4} m^3$	6.33×10^{-4} m^3		-29	
Surface Area	0.157 m^2	0.198 m^2		+26	
Static analysis					
Maximum Stress	181.8 MPa	181.7 MPa		≅ 0	
Maximum Displacement	8.270×10^{-2} mm	2.580×10^{-1} mm		+204	
Inertia	171 MPa	131.9 MPa		-23	
Thermal analysis					
Maximum temperature	323 ℃	322 ℃		≅ 0	
		XZ	XY	XZ	XY
First ring	241℃	226 ℃	179 ℃	-6	-25
Second ring	220 ℃	212 ℃	162 ℃	-4	-26
Third ring	195 ℃	199 ℃	149 ℃	+2	-24
Maximum heat flux	7×10^5 W/m^2	1.019×10^6 W/m^2		43	

On Table 3.12 are shown the results of both of the static analysis of the gas pressure. It is clear that the optimised piston uses more volume of the material, on the first line are shown the per cent of the volume above the 100 MPa, the optimised piston uses 5.85% of the material and the conventional uses only 0.51 % of the volume, which means that the optimised piston uses 10 times more material then the conventional piston. The second line is referred to tension above

75 MPa and the same conclusions are taken as well as the third line, where the tensions above 50 MPa are shown.

Table 3.12 Element volume used in the conventional and optimised piston

Element volume [%]		**Conventional piston**	**Optimised piston**
Conventional piston	**Optimised piston**		
0.51	**5.85**	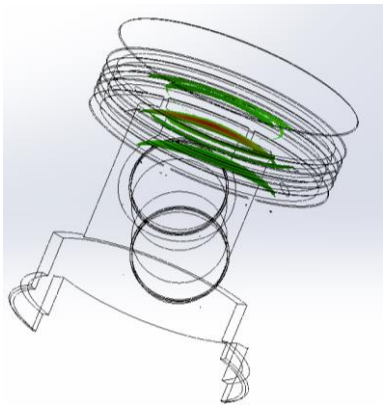	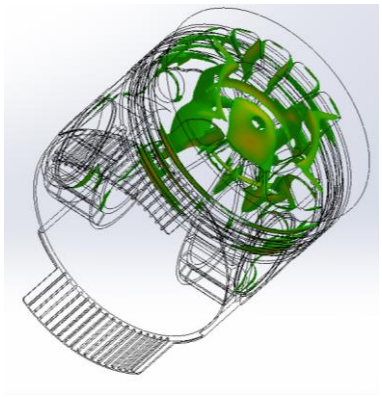
1.78.	**16.07**	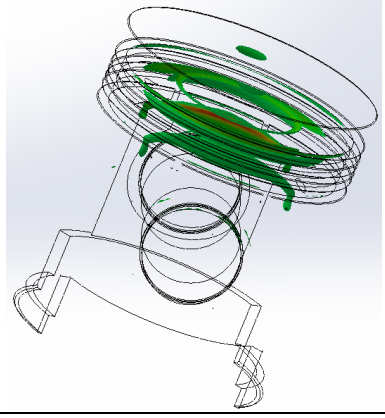	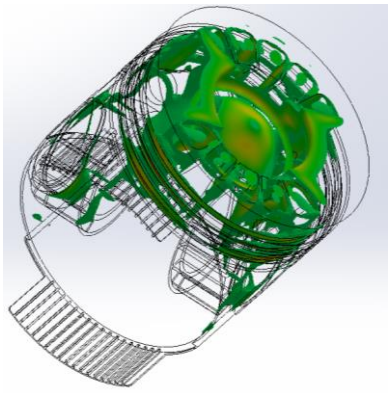
15.49	**44.30**	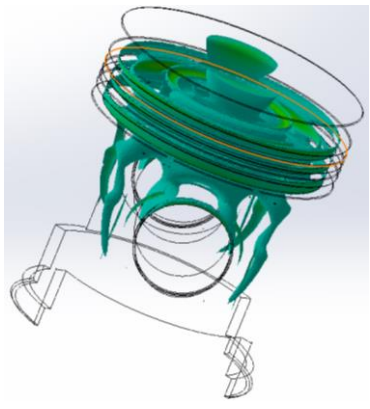	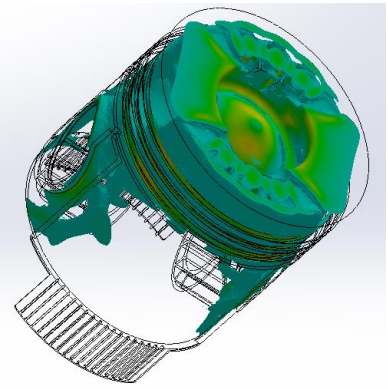

The Figure 3.45 shows the different maximum temperature results with different combustion temperature. The black bar is referred to the conventional piston while the grey bar represents the optimised piston. As it is observed the differences between them are not significant, although the optimised piston reaches values of maximum temperature lower than the conventional piston, in all of the cases.

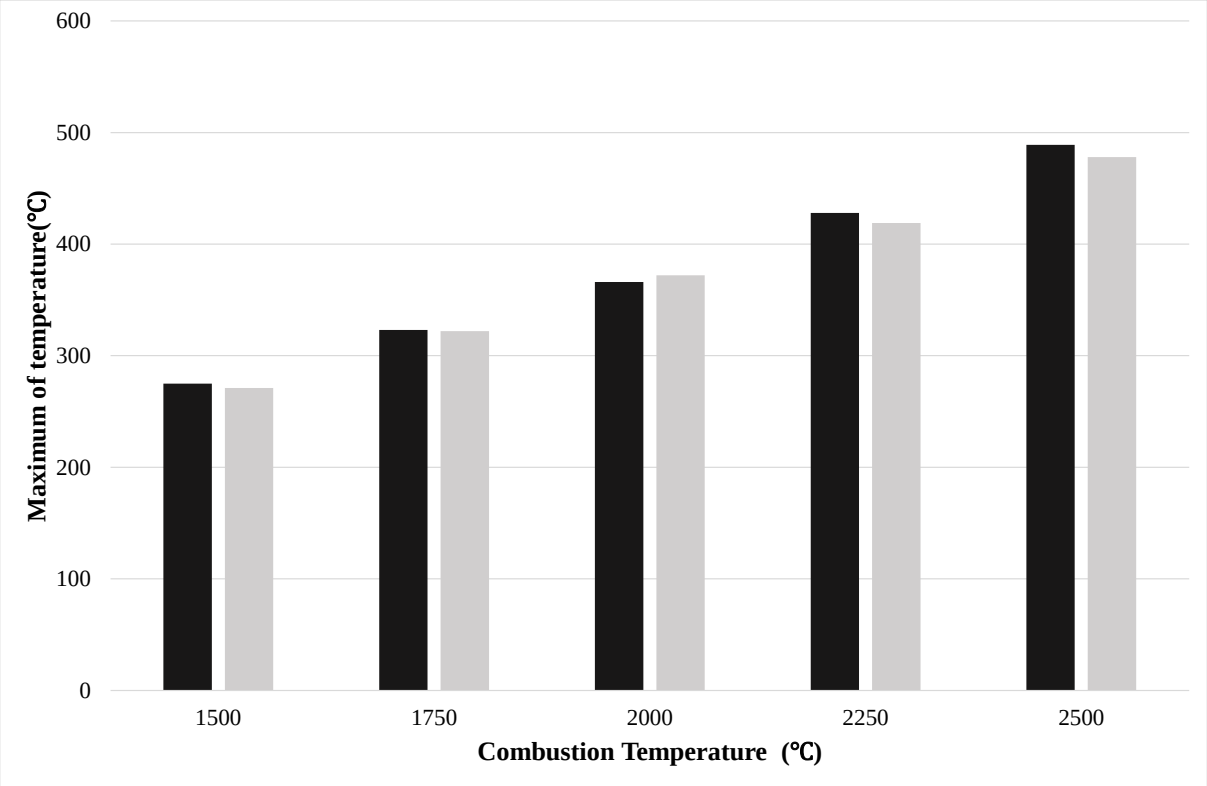

Figure 3.45 Maximum temperatures with different combustion temperatures

Either the optimised or the conventional piston reaches temperatures above 60% of the molten point of the aluminium alloy 4032 T6 when the combustion temperature is higher than 2000℃, which means that the maximum of the temperature that the material can stand is between 352 and 377 ℃, when the combustion temperature is higher than 2000℃ reaching temperatures of 428 and 419 ℃ when the combustion temperature is 2250℃, and 489 and 479 ℃ when the combustion temperature is 2500 ℃.

4. MANUFACTURE PROCESS

This chapter aims to explain the manufacture process. This process consists mainly in three parts.

The first part is to print both of the piston on a 3D printer machine. In the second stage, is used plaster to involve the 3D model previously printed, thereby creating a cavity with the same shape and pattern dimensions as the printing PLA (Polylatic acid) model. And finally the casting, where the melted aluminium is placed into the cavity formed by the prototype in the plaster. Only the first part of the manufacture process, the PLA model, will be explain on this chapter.[25]. The Figure 4.1 shoes, schematically, the stages of the manufacture process.

The first stage, "Design CAD model", was present on the previous chapter.

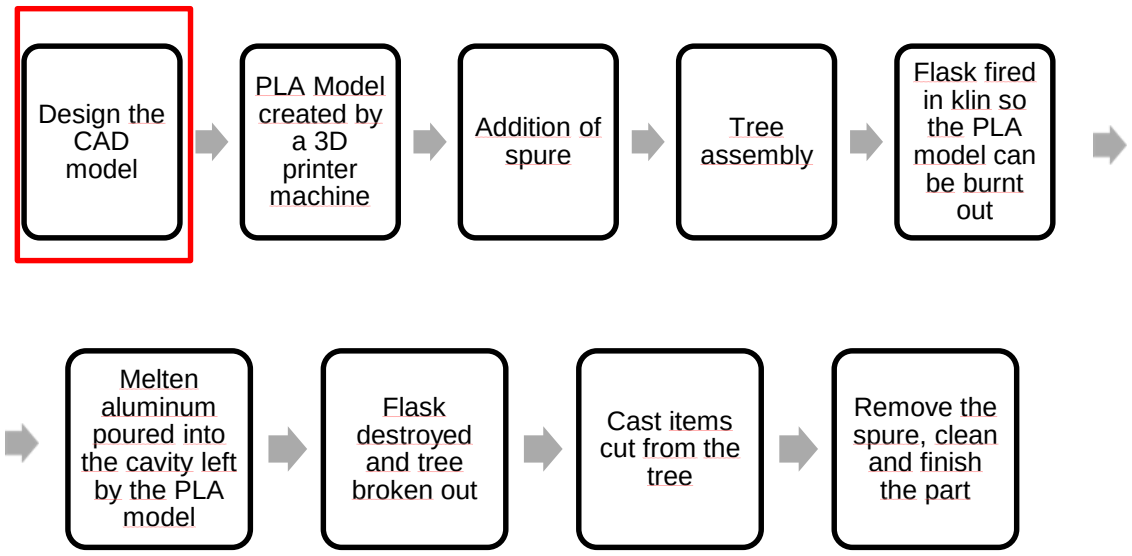

Figure 4.1 Manufacture process [25]

4.1 3D Printing

Before printing the pistons there were needed two steps. The first one was to try the thermal plaster cycle on the printing material, PLA. All of the material provided disappeared, without any ash, during the thermal cycle which proves that it is possible to use those PLA on this process. The first phase lasts 90 minutes and the temperature goes up to 150℃, the second stage is to remain at the same temperature, 150 ℃ for 180 minutes. Then, the temperature goes up at a gradient of 1.6 $℃/min$ until it reaches 730℃ for 360 minutes. The thermal cycle is present in Figure 4.2.

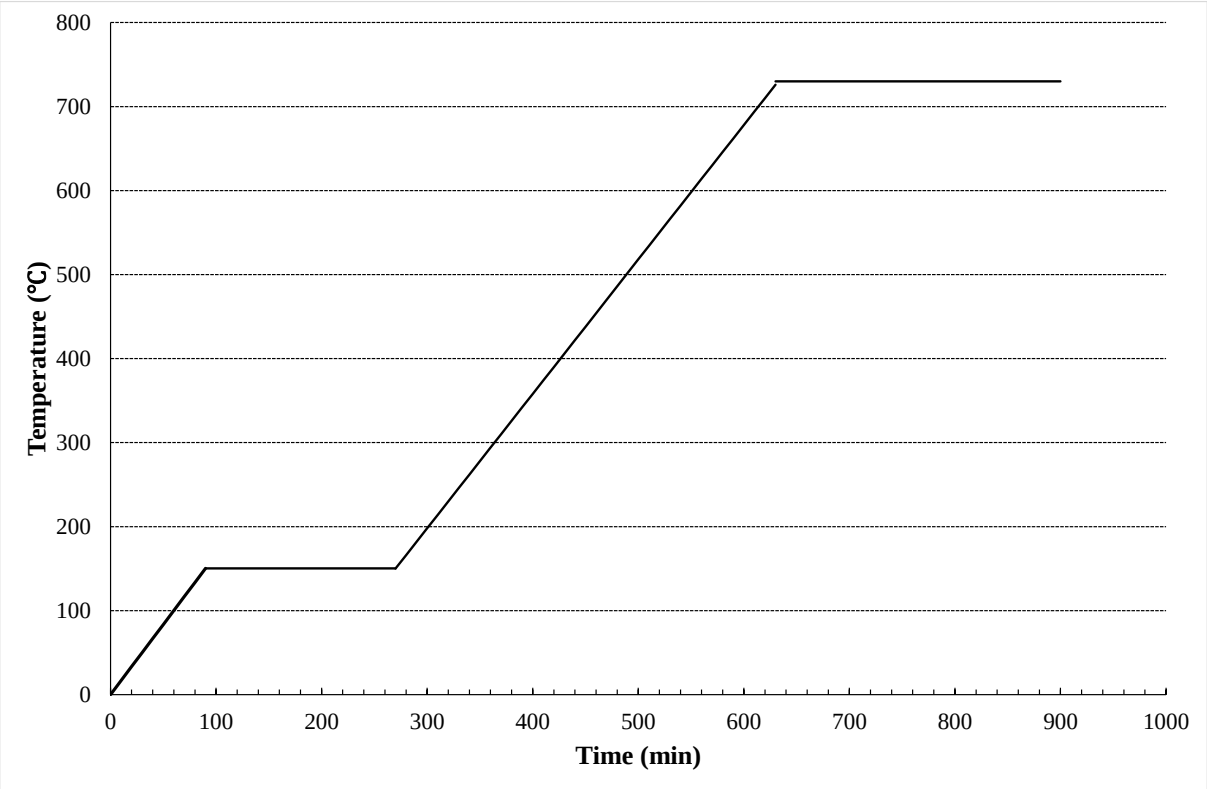

Figure 4.2 Plaster thermal cycle

The second step was to make some changes on the piston 3D model, due to some restrictions on the 3D printer machine, which is 0.4 millimetres, so the maximum thickness on the scale piston had to be at least 0.4 millimetres.

As it is shown on the next figure, the skirt has been changed. The fins were removed and it is consisted by a solid wall as the original one.

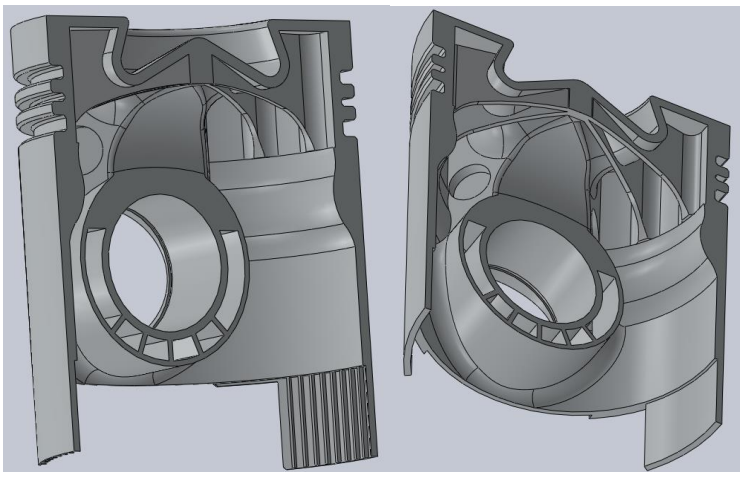

Figure 4.3 Skirt changed due to machine restriction

Another feature that had to be changed was the thickness on the piston boss wall, it is marked as red on the Figure 4.4. On the right the piston is without changes and on the left the piston has a thicker wall. The wall had an increase of 0.18 mm.

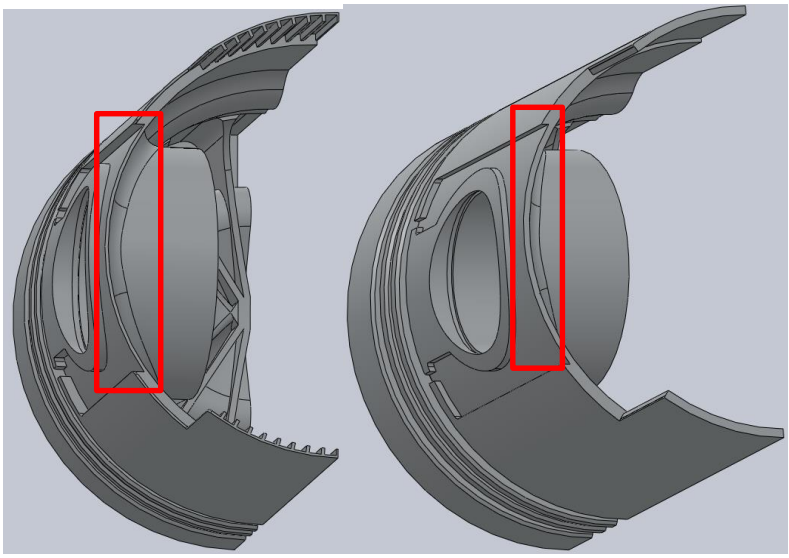

Figure 4.4 Pin boss wall

The mass of the optimised piston was increased due to the design changes, the difference of mass between the pistons is 25%.

4.1.1 Machine setup

After finishing all the alterations on the CAD design, the CAD file was save into a STL file, then, this file was transferred to CURA software and the piston was placed into the tray trough the software.

Later those changes, the machine was set up, see Figure 4.5, and the first 3D model was printed. The Figure 4.5, shows the place where the piston was printed.

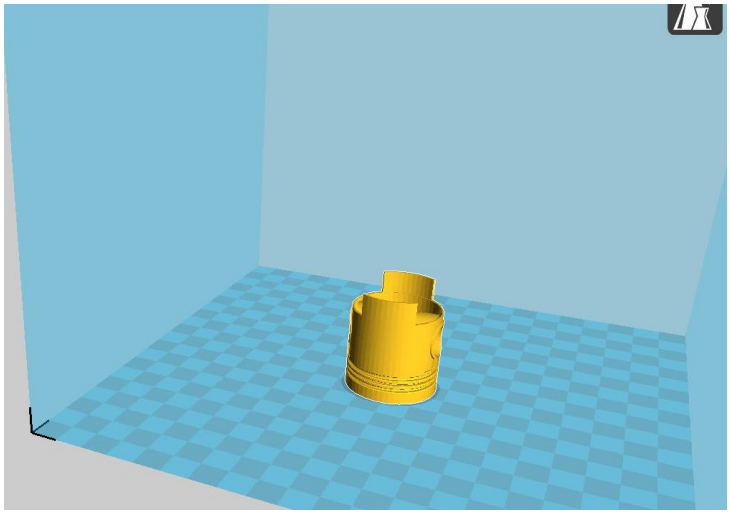

Figure 4.5 Piston placement

The Figure 4.6 shows the machine set up, sush as the layer height which is correlated with the size of each layer of material, in this case is 0.1mm. Thinner slices produce a smoother pattern surfaces. The nozzle size, 0.4 mm, that was the reason of the main changes on the modelling. The suports were used on the piston chamber as in the piston boss feature.

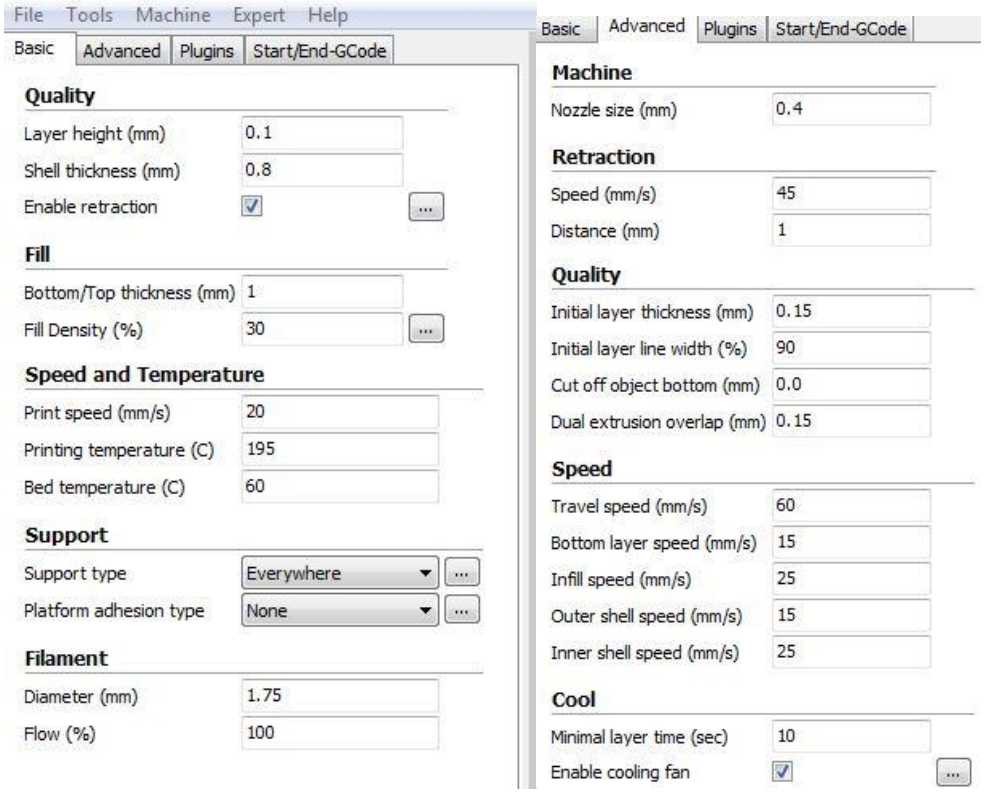

Figure 4.6 Machine Setup

The build process is mostly automatic. Each layer is usually about 0.1 mm thick, though it cannot be thinner than that. The whole process took 4 hours for each PLA model. On Figure 4.7 it is possible to see how the PLA tis made on the interior. It is made with an inner net in order to minimize the possibility of having ash during the burnt out process.

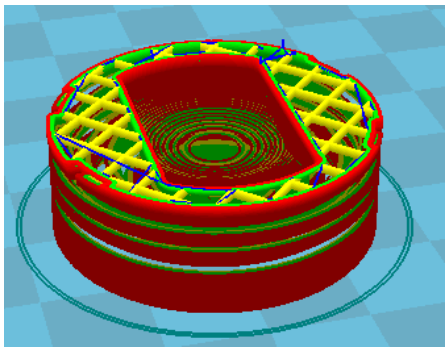

Figure 4.7 Inner side of the PLA model

Each machine has its own requirements for how to prepare for a new print part. This includes refilling the polymers, binders and other consumables the printer will use. It also covers adding a tray to serve as a foundation or adding the material to build temporary water-soluble supports. The first attempt of PLA pistons was not succeed due to the support automatically built on the software Cura. On the right side we can see the optimised piston, the problem here was the overheated support whist stuck on the combustion chamber. On the left we have the conventional piston, the support was not properly printed which crated a damaged combustion chamber.

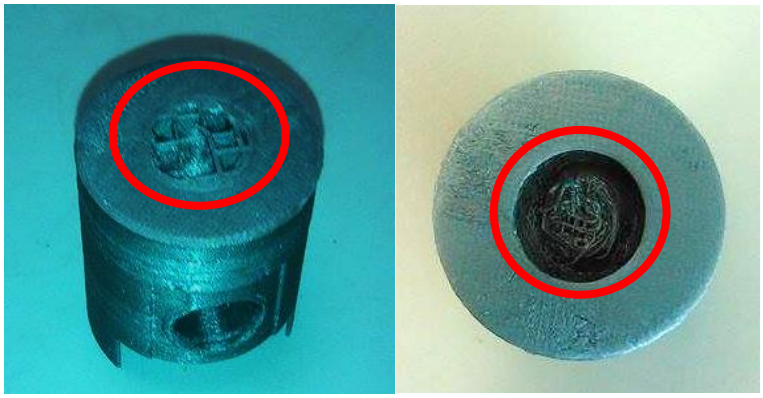

Figure 4.8 Problems with the support

So the solution was to draw a new support, a small cone, on SolidWorks™, instead of using the software pre-defining support, Figure 4.9. There were two trials, the first, as it is show on Figure 4.9was not succeed. Then a second support, with eight beams.

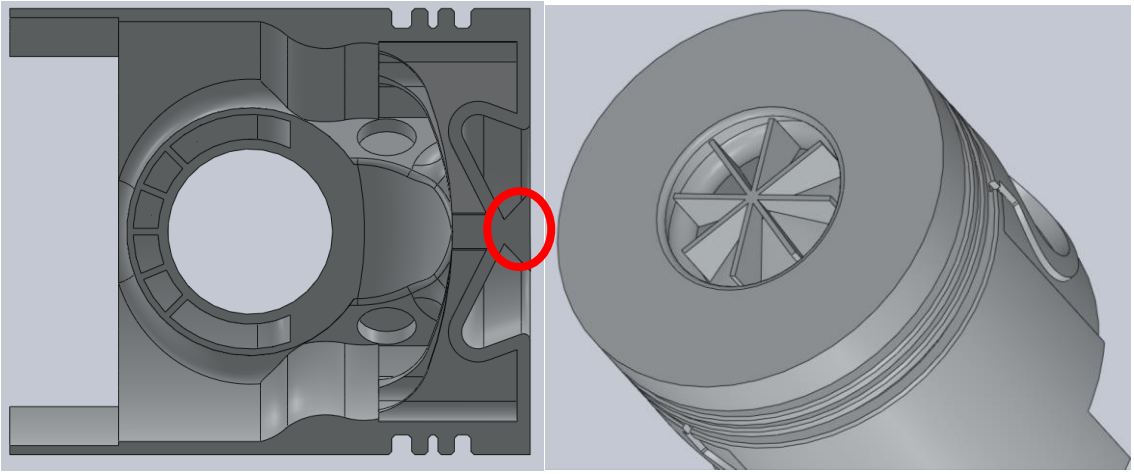

Figure 4.9 3D printer support

The support was removed with a dremel, as it is possible to see in Figure 4.10 the surface finish is not perfect, especially on the piston chamber where some scratches have been left due to the support removal.

Figure 4.10 Piston chamber, PLA model

On the Figure 4.11 the inner side of the PLA pistons is shown. The finish surface of the PLA model is not perfect due to the layer size of 0.1mm, it is possible to observe some stripes, and each stripe means one layer of material. The aluminium model will get the same pattern.

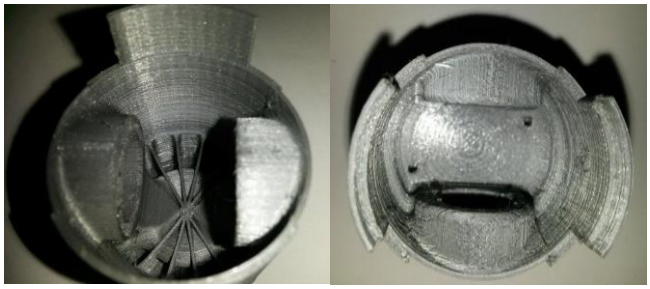

Figure 4.11 Inner side of the PLA piston

5. CONCLUSIONS AND FUTURE WORK

This chapter intends to present the conclusions of this dissertation, on the first section, and on the second section the future work.

5.1 Conclusions

The following section will describe the main conclusions that were taken during this dissertation. The conclusions are made through the methodology, each step of the methodology is analysed and the conclusions are taken. It starts with de design and goes until the beginning of the manufacture process.

5.1.1 Design

The main goal of this optimization is to reduce mass on a specific component, a piston, without changing the outside geometry.

Investigating the stress contour of the piston FEA model during the expansion of the gases showed the same locations present lower stresses such as the lower part of the piston boss and the skirt, which means that those locations are suitable to design changes.

The design optimisation was performed with an iterative process which requires a big amount of time. Each design change requires a static analysis and each time that is needed to make a static analysis is required a new mesh. There were two solutions for the pin boss, one with a cellular structure, which was not possible to simulate, and the other one with ribs, where the simulation was performed.

5.1.2 Static analysis

The static analysis have shown that both of the pistons have the same maximum of stress (182 MPa), it has also shown that the maximum is placed in the same area, above the piston boss. The factor of safety at is minimum is the same, because the highest stresses are the same in both of the pistons.

The static analysis was only performed on a piston, however inserting the others components, such as the connecting rod and the pin, the results can be different.

The displacement is greater on the optimised piston, the lateral force on the skirt was not tested which can leads to different results on the displacements.

5.1.3 Inertia

The weight reduction of the piston also reduces the inertia, which means the tensile force stressing (stretching forces) of the connecting rod and crankshaft are significantly lower allowing the use of lighter components throughout the engine powertrain. The inertia was reduce in 23%, despite of the reduction of weight on the piston of 29% the inertia depends on the total of mass, the piston mass and the rod mass, the rod mass is the same in both of them, that is the reason why the inertia only drops 23%.

5.1.4 Thermal analysis

The thermal analysis have shown that the maximum of the temperature is basically the same, which means that is possible to keep the same thermal requirements without a gallery, however the heat flux is higher on the optimised piston, which can lead to a crack of the oil.
The optimised piston has different temperatures on the ring lands depending on the direction which can leads to thermal stresses, while the conventional piston presents the same temperature on the rings.
Neither the pistons, the conventional nor the optimised, can endure temperatures above the 2000℃, which means the range of temperatures is only 250 ℃ in both of them.

5.1.5 Manufacture process

The proposed manufacture process is to slow for the manufacture requirements. Each model, scale to one quarter of the original size, takes, at least, 4 hours, to build if the model was built on tis original scale the process would take a lot more time. The finishing of the PLA model is not perfect, so whether the 3D printer is capable of printing a better PLA model or the final aluminium component requires a machining finish operations.
The plaster cycle takes 12 hours to be finished.
The process of manufacture was not finished, so further conclusions cannot be taken.

5.2 Future work

Develop a new method to optimise components. The method that was used during this dissertation is longstanding. The developing of a new method should take the maximum of static analysis and establish as a limit for the new design, so that the person whom is responsible for the design does not have to simulate at each time the he does some design change. The new method should be an algorithm with boundary conditions and the desire output values.

Run the static and thermal analysis of the piston with the cellular structure.

Apply and study different cellular structures on simpler components, and test them physically with aluminium models.

Study the effect of the heat flux on the oil. The oil loses thermal properties with an increase of the temperature. Those properties were not studied, but they are important to the thermal transference field.

Apply different techniques of optimization, such as topological optimisation and shape optimisations and combine them.

Cast the pistons and test both of them with thermal and mechanical loads.

Cost analysis of the manufacture process.

BIBLIOGRAPHY

[1] C. K. Meyers Marc, *Mechanical Behavior of Materials*, Second edi. 2008.

[2] N. a. Meisel, C. B. Williams, and A. Druschitz, "Lightweight Metal Cellular Structures via Indirect 3D Printing and Casting," *Solid Free. Fabr. Symp.*, pp. 162–176, 2012.

[3] P. Pinto, N. Peixinho, F. Silva, and D. Soares, "Compressive properties and energy absorption of aluminum foams with modified cellular geometry," *J. Mater. Process. Technol.*, vol. 214, no. 3, pp. 571–577, 2014.

[4] F. S. Silva, "Fatigue on engine pistons - A compendium of case studies," *Eng. Fail. Anal.*, vol. 13, pp. 480–492, 2006.

[5] S. Bennett, "Modern Diesel Technology: Diesel Engines", 2009.

[6] MAHLE Gmbh (Ed.), Ed., "*Pistons and engine testing*." 2012.

[7] F. Z. Se, L. Block, Q. C. Tribosil, G. D. Casting, G. D. Casting, and I. Diesel, "AAM – Applications – 1 Power train Contents", 1995.

[8] K. S. A. Pistons, "Kolbenschmidt Pierburg Group KS Aluminum Pistons."

[9] H. M. and K. S. Arnd Baberg, Marcus Freidhager, "Aspects of Piston Material Choice for Diesel Engines," pp. 26–30, 2012.

[10] E. A. Association, "Manufacturing – Casting methods," *Alum. Automot. Man.*, 2002.

[11] N. Materials, "Kolbenschmidt Pierburg Group New Materials and Processes.", 2006

[12] J. Martins, "*Motores de Combustão Interna"*, 2ª edição. Publindústria, 2006.

[13] Kolbenschmidt Pierburg Group, "Technical Information," pp. 2–4, 2012.

[14] R. Cited and C. Ribeiro, "(12) United States Patent (16) Patent N6 ;," vol. 2, no. 12, 2013.

[15] R. K. Rajput, "Internal Combustion Engines," pp. 224–261, 2005.

[16] M. Ranjbarkohan, M. Rasekh, A. H. Hoseini, and K. Kheiralipour, "Kinematics and kinetic analysis of the slider-crank mechanism in otto linear four cylinder Z24 engine," *J. Mech. Eng. Res.*, vol. 3, no. 3, pp. 85–95, 2011.

[17] D. Joseph, *Metals handbook- Properteies and selection of metals*, 8 th. 1961.

[18] "Soliworks. Help Simulation static analysis." 2013.

[19] E. I. Analysis, "4 Mesh Control in SolidWorks Simulation," pp. 65–73, 2012.

[20] "Finite element mesh generation methods : a review and classification," vol. 20, no. I, pp. 27–38, 1988.

[21] University of Florida, "0.1. Failure Theories," pp. 3–10, 2006.

[22] T. S. Prakash, V. District, and A. Pradesh, "Investigation of Two Engine Pistons by FEA," no. 11, pp. 1217–1221, 2014.

[23] A. K. Agarwal and M. B. Varghese, "Numerical investigations of piston cooling using oil jet in heavy duty diesel engines," *Int. J. Engine Res.*, vol. 7, no. 5, pp. 411–421, 2006.

[24] J. C. Teixeira, “Apontamentos de Transferências de calor-Convecção,” pp. 84–87, 2002.

[25] J. Campbell, “Complete Casting Handbook,” pp. 911–938, 2011.